MEASUREMENTS OF PARAMETERS OF A FLASHLAMP PUMPED ALEXANDRITE LASER

BY

DAVID CHARLES RIDER

Bachelor of Science

Oklahoma State University

Stillwater, Oklahoma

1993

Submitted to the Faculty of the Graduate
College of Oklahoma State University
in partial fulfillment of
the requirements for
the Degree of
MASTER OF SCIENCE
December, 1998

MEASUREMENTS OF PARAMETERS
OF A FLASHLAMP PUMPED
ALEXANDRITE LASER

Thesis Approved:

Thesis Advisor

Wayne B. Powell
Dean of the Graduate College

ACKNOWLEDGMENTS

I would like to convey my appreciation to the professors and staff of the electrical engineering department for their support and guidance during my studies. I would also like to express my sincere appreciation to Dr. Jerzy Krasinski first and foremost, as well as Dr. Czeslaw Radzewicz for their patience, understanding and wisdom as well as assistance during my research. I have learned a great deal and profited in many ways from their friendship and tutelage. It has been an honor to have been one of their pupils.

TABLE OF CONTENTS

Chapter

Appendices

LIST OF FIGURES

Figures

Figures, cont.

Figures, cont.

CHAPTER II

POWER SUPPLY SYSTEMS

FLASHLAMP IONIZING SUPPLY (13.5 kV)

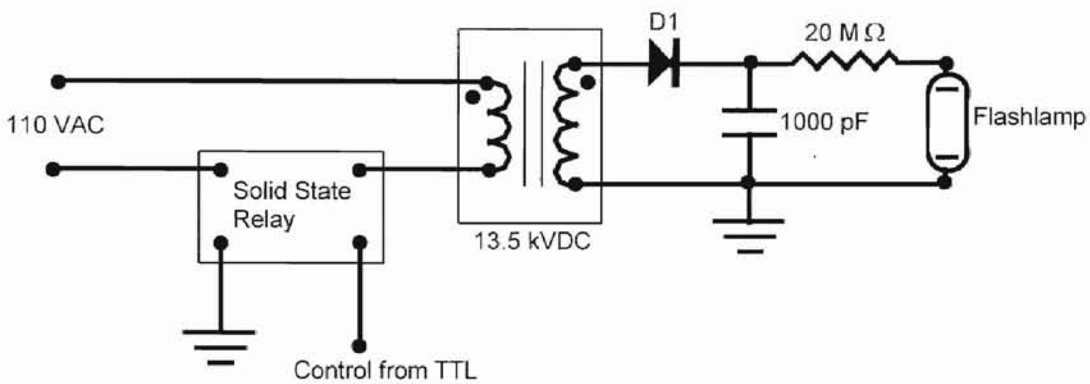

Figure 1

13.5 kV Flashlamp Ionizing Circuit.

During the startup phase of the laser, a 13.5 kV power supply is used to ionize the flashlamp. Once the gas has been ionized, the simmer circuitry supplies a small current through the flashlamp which maintains a lower resistance across the flashlamp, keeping the lamp "alive" during the firing phase of operation. Once the flashlamp is ionized and the simmer power supply takes over, the ionizing power supply is turned off by the TTL controls and if desired, also by the user. Figure 1 shows the ionizing (13.5 kV) power supply circuit diagram. The output voltage of the power transformer is sinusoidal (AC). To convert the AC output to a positive output voltage, a half-wave rectifier circuit composed of two parallel 500 pF/30 kV capacitors and a high voltage diode (D1) were used. The ionizing power supply should never be on when the mercury relay is engaged to insure that high voltage is not applied to the firing circuitry. The TTL circuitry checks for this condition and will not permit this state to occur.

The 13.5 kV supply has a solid state relay attached which allows the TTL controls to switch the supplies on or off according to the input from the user. This control relay is operated by a 5 V DC low current (3 mA) signal from the TTL. An opto-coupler is located between the relay and the TTL to protect the TTL from feedback and damage. This relay is manually controlled by the user with the TTL acting as the watchdog to eliminate the possibility of system damage.

SIMMER SUPPLY

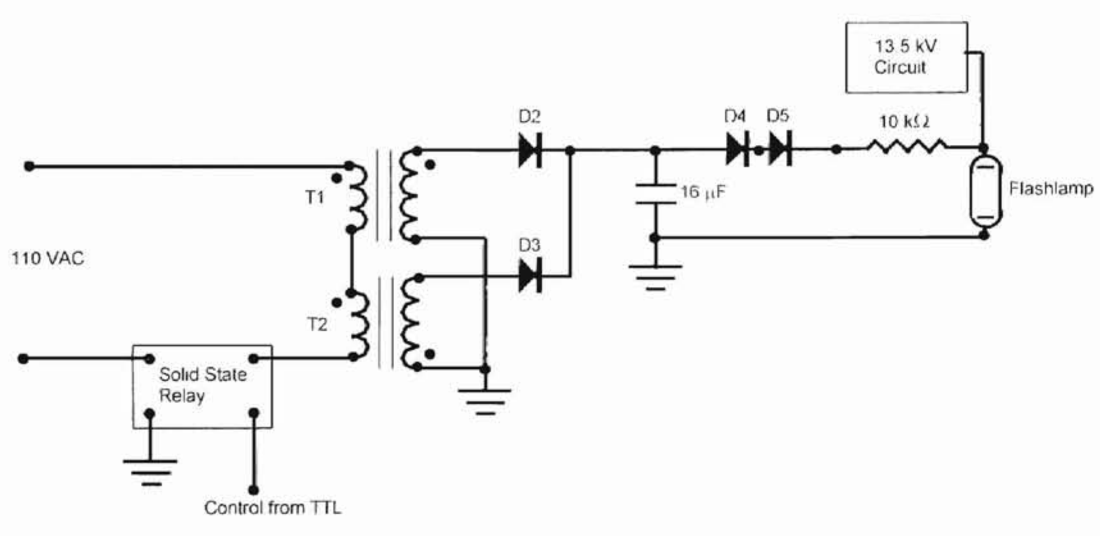

Figure 2

Simmer Supply Circuit.

The simmer supply is basically a DC supply which maintains the 100 mA simmer current through the flashlamp. Figure 2 shows a diagram of the simmer supply. The simmer supply consists of two transformers, two diodes, and two capacitors, and converts single phase 110 V AC to a DC voltage. When 110 V AC is applied to the primary windings, the transformer's secondary output is rated at 1.8 kV AC and 225 milliamperes (mA). The transformers are configured such that the primaries are in series while the secondaries are in parallel. One of the secondaries is 180^0 out of phase with its primary, and therefore also 180^0 out of phase with the other transformer's secondary output. A high voltage diode is on each of the secondary outputs (D2, D3), with two 8 μF capacitors in parallel (equaling a total of 16 μF) connected across the diode outputs and ground. This configuration provides full-wave rectification at the supply's output. The output is approximately 900 V in the parallel connections of the secondary windings, providing a suitable voltage for the desired system as well as the ability to handle a larger circuit load. The simmer supply circuitry is protected from the 13.5 kV supply via two high voltage diodes in series (D4, D5). The simmer supply is also connected to power through a solid state relay and is controlled by the user and TTL in a similar fashion to the aforementioned 13.5 kV supply.

RCS-1500 POWER SUPPLIES

Two RCS-1500 Capacitor Charging Power Supplies, manufactured by Converter Power, Inc., are used in parallel in a master/slave configuration in order to charge the

50 μF capacitor bank. The RCS-1500 power supplies are high power current sources which are specifically designed to charge capacitors at a constant rate. Each RCS-1500 has a rated output power of 1500 Joules/second and operates from a nominal 220 V AC input line. At rated output, it takes 33 milliseconds to charge the 50 μF capacitor bank at a charging voltage of 1,400 V. The capacitor bank is composed of ten 5 μF low induction capacitors to enable it to store up to 50 J of energy. The capacitor bank is charged to a voltage set by the user which enables it to deliver the selected energy to the flashlamp.

SILICON CONTROLLED RECTIFIERS

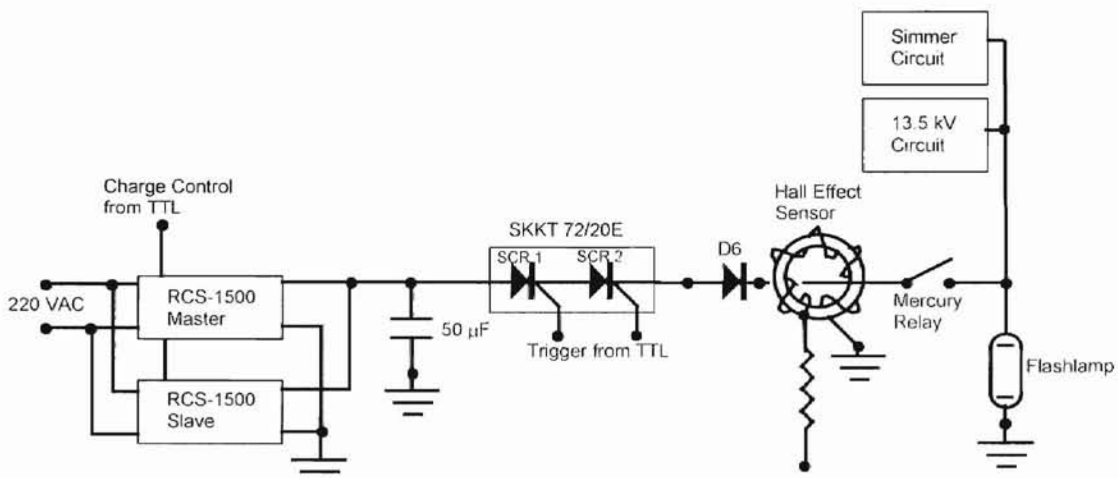

Figure 3

Firing / Charging Circuit.

Silicon controlled rectifiers (SCR) are used for isolation and switching of the 50 μF capacitor bank voltage. Once triggered, the SCRs connect the capacitor bank to the flashlamp until the 50 μF capacitor bank is discharged. Once the current stops flowing from the capacitor bank, the SCRs open allowing the capacitor bank to be recharged. Two 1:1 pulse transformers are used to provide isolation between the SCRs' gates and the pulse generation circuit. Fast switching diodes are placed across the transformers to allow energy dissipation of possible transients. A 1700 V varistor protects the SCRs, RCS-1500s, and the simmer supply should the isolating high voltage diode fail. Figure 3 shows the firing/charging circuit which contains the SCRs along with the 50 μF capacitor bank and the RCS-1500s.

TTL CONTROLLED RELAYS

A mercury relay is used to disconnect the section of the system containing the flashlamp, the 13.5 kV power supply, and the simmer power supply from the firing/charging circuit. The mercury relay isolates the firing/charging circuit from the high voltages generated by the flashlamp ionizing power supply during the initial flashlamp ionizing procedure. The TTL controls ensure that the 13.5 kV supply will not energize if the mercury relay is engaged, thereby preventing accidental damage to the firing/charging circuit and supplies.

CAPACITOR BANK DISCHARGE CIRCUIT

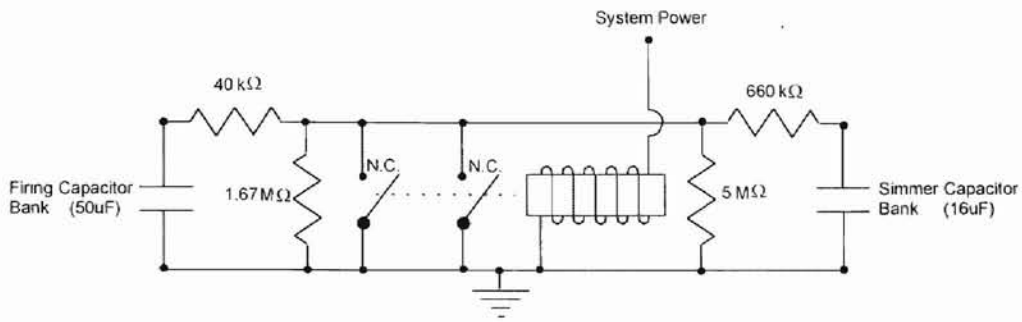

Figure 4

Capacitor Bank Discharge Circuit.

A fourth relay which is a normally closed DPDT (Double Pole Double Throw) is used to automatically discharge the capacitor banks to eliminate a safety hazard due to leaving the capacitors charged to a large voltage. Figure 4 shows the capacitor bank discharge circuit. This relay opens during normal operation of the system via a 24 V signal and closes when either the system is switched off or power is lost. When the relay closes, the 16 μF simmer capacitor bank discharges through a resistance of 660 kΩ, resulting in a time constant of 10.6 seconds which enables the bank to discharge in approximately one minute. At the same time, the 50 μF firing capacitor bank is also allowed to discharge through a 40 kΩ resistance producing a time constant of two seconds which results in an approximate ten second discharge time for the bank.

If the aforementioned capacitor discharging relay fails in some manner and the capacitor banks are not automatically discharged, the banks will be discharged through resistors which are permanently connected from each bank to ground. The 16 μF capacitor bank is connected to ground through a 5 MΩ resistance. This combination provides a time constant of 80 seconds. The 50 μF capacitor bank is connected to ground through a 1.67 MΩ resistance. This combination provides a time constant of approximately 83 seconds. The large time constants were chosen to ensure that no significant leakage occurs during operation of the system.

FLASHLAMP SIMMERING VOLTAGE METER

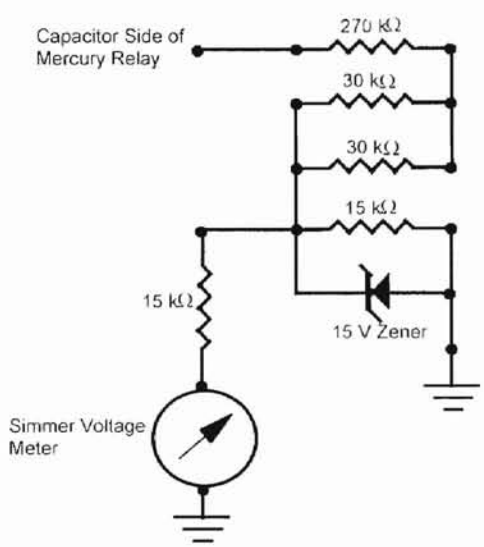

Figure 5

Flashlamp Voltage Meter Circuit.

The flashlamp simmering voltage is monitored by the control system and is displayed on the front panel of the power supply with a range of 300 V. A voltage divider is utilized to scale down the actual voltage at the flashlamp to a voltage range compatible with the 15 V panel meter. A signal is read from the voltage divider between a 275 MΩ resistor and a 15 kΩ resistor which is then fed through a 15 kΩ resistor to the meter. The meter's scale was modified to display the actual voltage across the flashlamp (0 to 300 V). Figure 5 shows the voltage circuit.

COMPARATORS

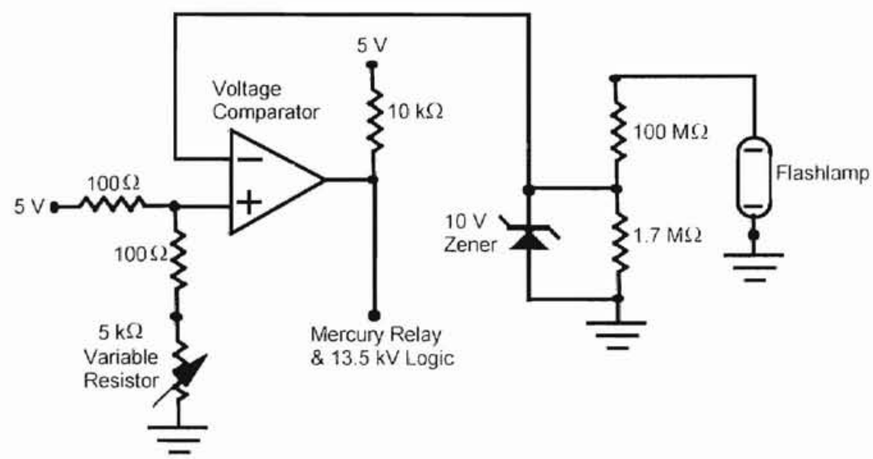

Figure 6

Flashlamp Voltage Comparator Circuit.

In addition to the aforementioned voltage divider, a second voltage divider scales down the voltage at the flashlamp to a voltage compatible for use as an input to a comparator. Figure 6 shows the flashlamp voltage comparator. The comparator determines if the voltage at the flashlamp is above or below the desired threshold voltage. The threshold voltage is determined by setting the reference voltage, which is adjusted via a potentiometer located on the TTL circuit board. This comparator is used to control the supply power to the 13.5 kV power supply. The voltage signal for the comparator is read from the voltage divider between the 100 MΩ and the 1.7 MΩ resistors. The large resistance (100 MΩ) allows only a very small current to be diverted through the voltage divider so that the flashlamp load is not significantly affected. A 10 V zener diode is used as protection for the comparator and prevents high voltages which would cause damage from being applied to the comparator.

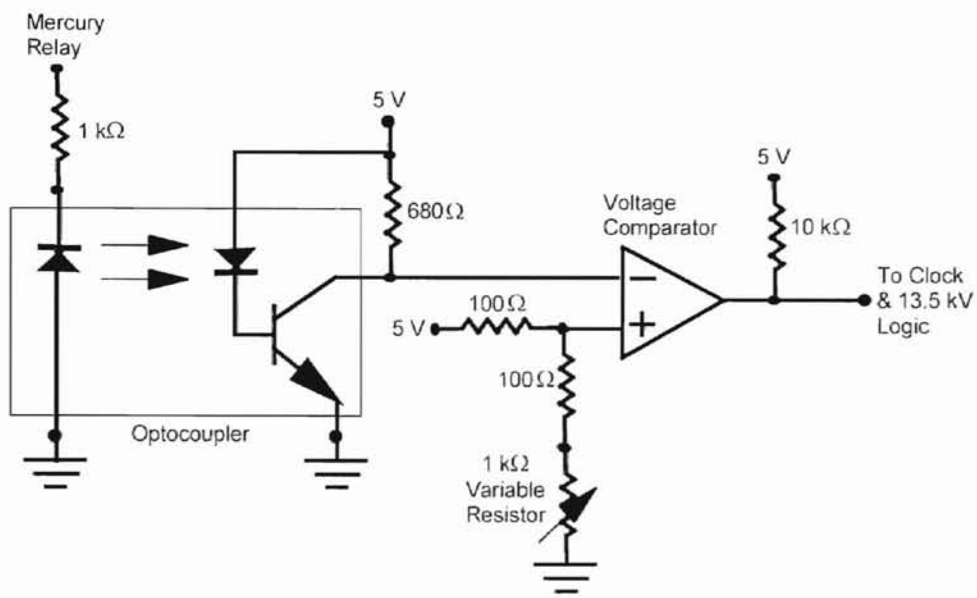

Figure 7

Mercury Relay Test Comparator Circuit.

A second voltage comparator is implemented on the input side of the mercury relay and is used to enable/disable the clock/firing circuitry and disable/enable the 13.5 kV supply. This comparator is shown in Figure 7.

HALL EFFECT CURRENT SENSOR

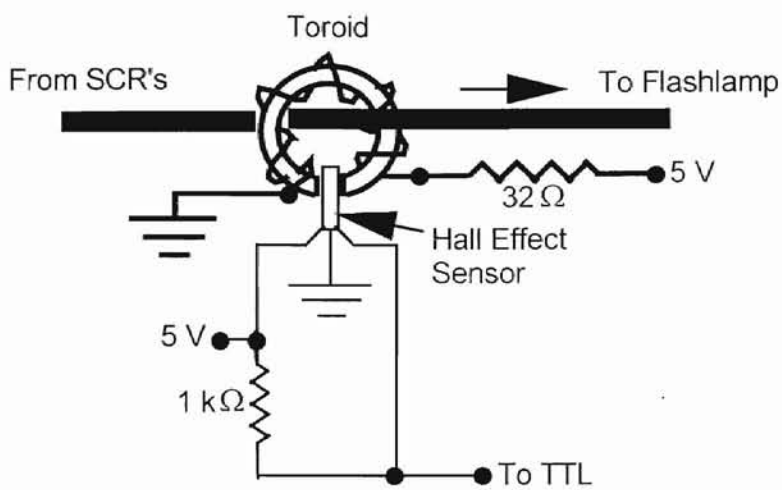

Figure 8

Current Sensor Circuit.

A Hall effect sensor is used to detect current in the conductor from the 50 μF capacitor bank to the flashlamp. Figure 8 is a diagram of the Hall effect sensor and toroid circuit. The Hall effect sensor is a device used to detect magnetic fields. In the presence of a magnetic field, a switch closes inside the sensor. An opposing magnetic field is necessary to cause the sensor to switch back to an open state.

The sensor is placed in a short air gap of a toroid in order to increase the device's sensitivity. A constant magnetic field is created by supplying 5 V DC to a wire wrapped around the toroid to keep the Hall effect sensor in a closed state unless the flashlamp is fired.

The conductor from the 50 μF firing capacitor bank to the flashlamp is passed through the toroid. When the flashlamp is fired, the flashlamp current in the conductor creates a magnetic field which opposes the constant magnetic field already present in the toroid. The magnitude of the flashlamp-generated magnetic field is much greater than the static magnetic field and therefore causes the Hall effect sensor switch to open. The Hall effect switch remains open until the current through the flashlamp decreases to zero.

FLASHLAMP CURRENT PULSE CONDITIONING

After triggering the SCRs, a large amount of energy from the 50 μF firing capacitor bank is delivered to the flashlamp in the form of a current pulse. This current pulse lasts for approximately one hundred microseconds but has a rather large peak amplitude of approximately 400 A. These high amplitude short pulses create a shock wave within the flashlamp gas which can shorten the flashlamp's lifetime and cause damage. Flashlamp lifetime depends on how large the current pulse amplitude is and how abrupt the transition from the simmer current level to the maximum peak current during the firing of the flashlamp [3]. Therefore, to increase the flashlamp's lifetime, a saturable inductor was introduced into the flashlamp's firing circuit. The conductor which is connected between the flashlamp and the 50 μF firing capacitor bank is looped four times around a Metglass [4] core. Figures 9 and 10 show the difference in the initial rate of rise from simmer current amplitude to the maximum current amplitude for one loop and four loops (operational setup) around the Metglass core. When the flashlamp is

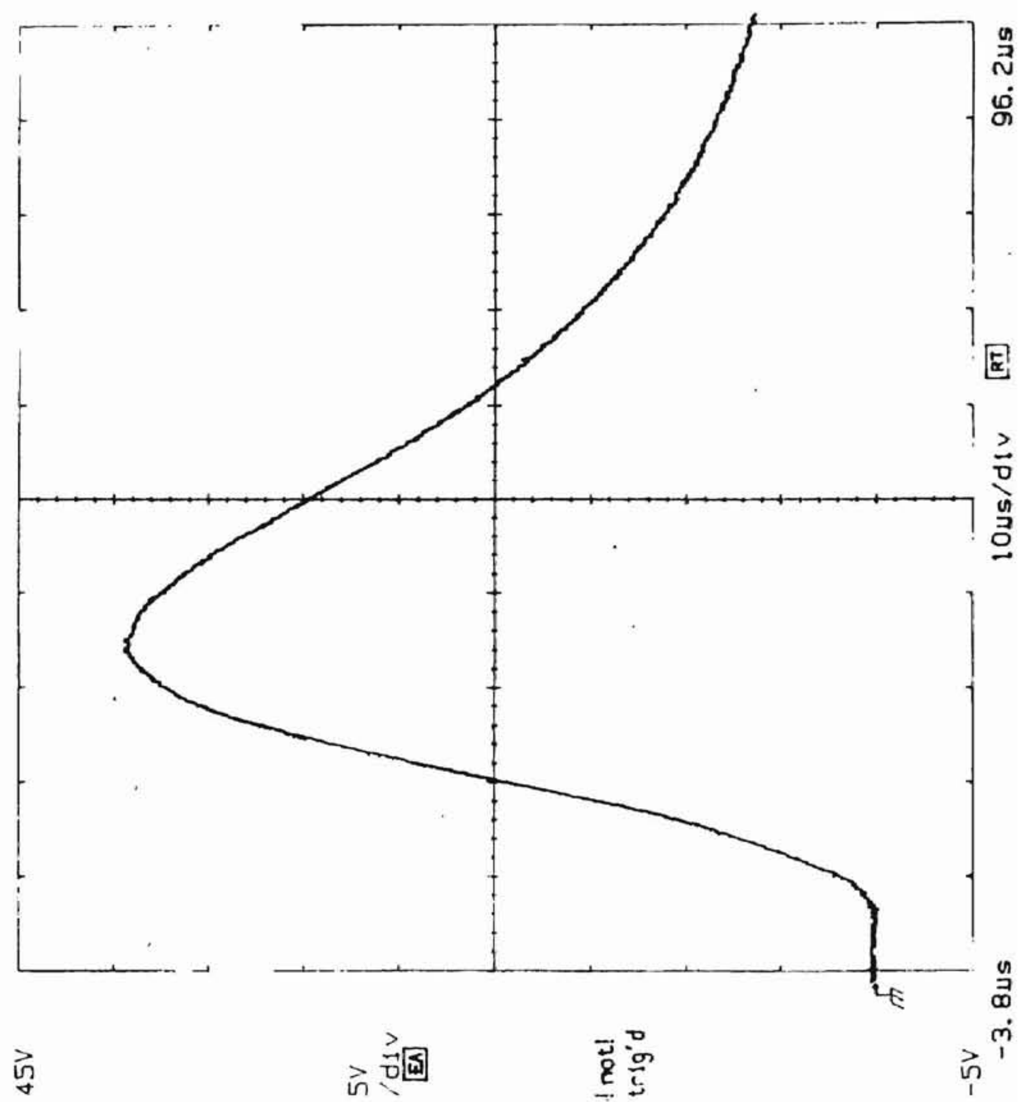

Figure 9

Current Pulse through one loop three core circuit at 800 V with simmer.

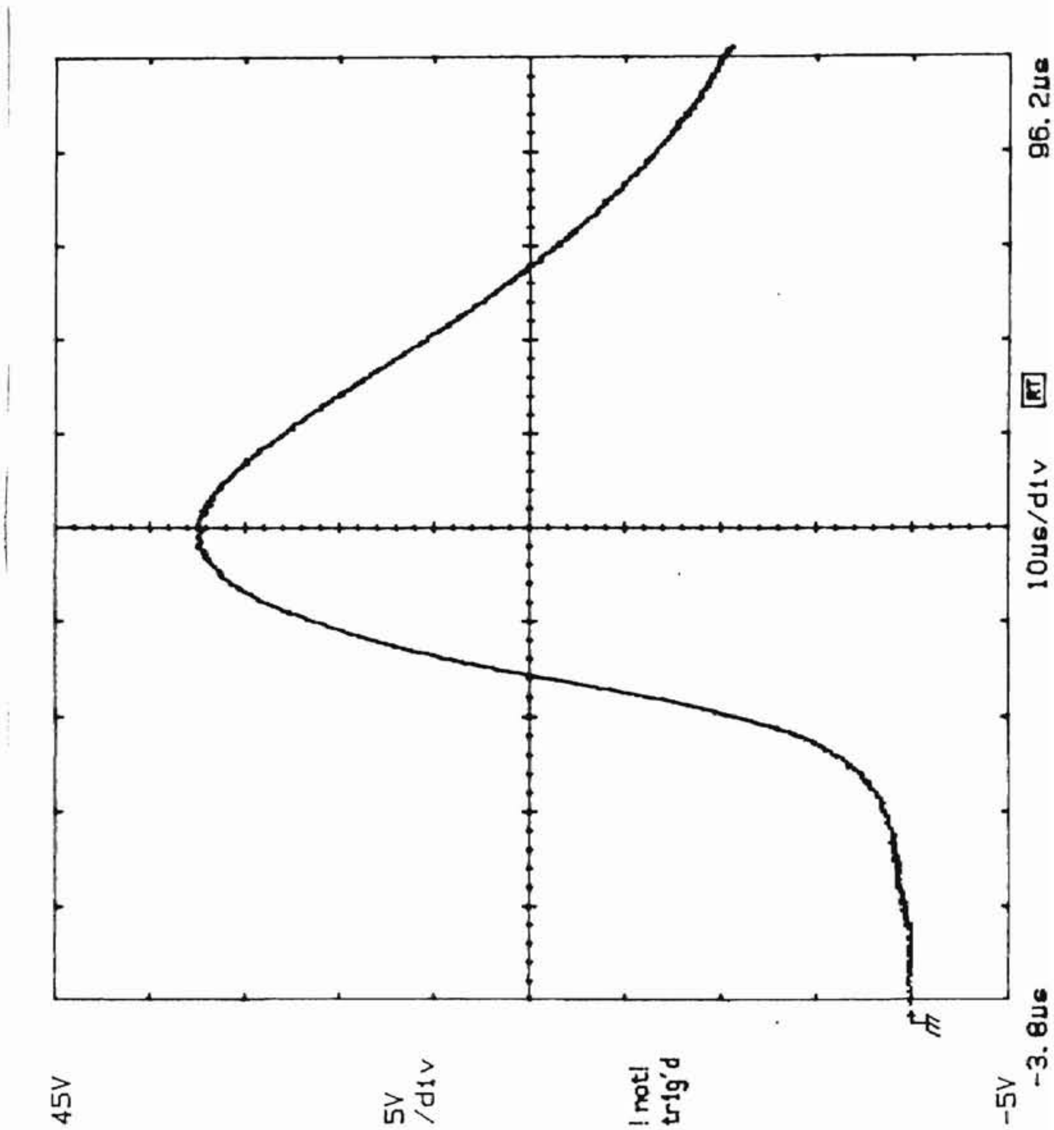

Figure 10

Current Pulse through four loop three core circuit at 800 V with simmer.

fired, the core is in the unsaturated high magnetic permeability state resulting in large inductance of the coil. This slows the rise time of the leading edge of the current pulse. The decrease in rise time "softens" the leading edge reducing the shock wave amplitude. Once the Metglass inductor is saturated, the inductance of the coil is reduced to a very small value and the rate of current rise increases, allowing short pulse generation, which is unaffected by the presence of the inductor. After the pulse, the core is remagnetized in the opposite direction by using the current provided by the simmer supply. The current flows through a small coil wrapped around the core and prepares the core for the next pulse. Appendix C shows the current pulses resulting from the various different inductor/wiring configurations tested.

TTL CONTROLS

TTL circuitry is used for controlling different aspects of the power supply system. The TTL controls allow for the proper laser operation while also providing safeguards so that improper and potentially damaging system conditions do not occur, whether it be operator error or a system failure. Appendix B shows the control system flowchart which details the system's conditions and corresponding responses.

POWER SUPPLY

The system components previously described are enclosed in a stand alone cabinet separate from the laser it drives. Figure 11 is a photograph of the completed and operational flashlamp pumped laser power supply/controller.

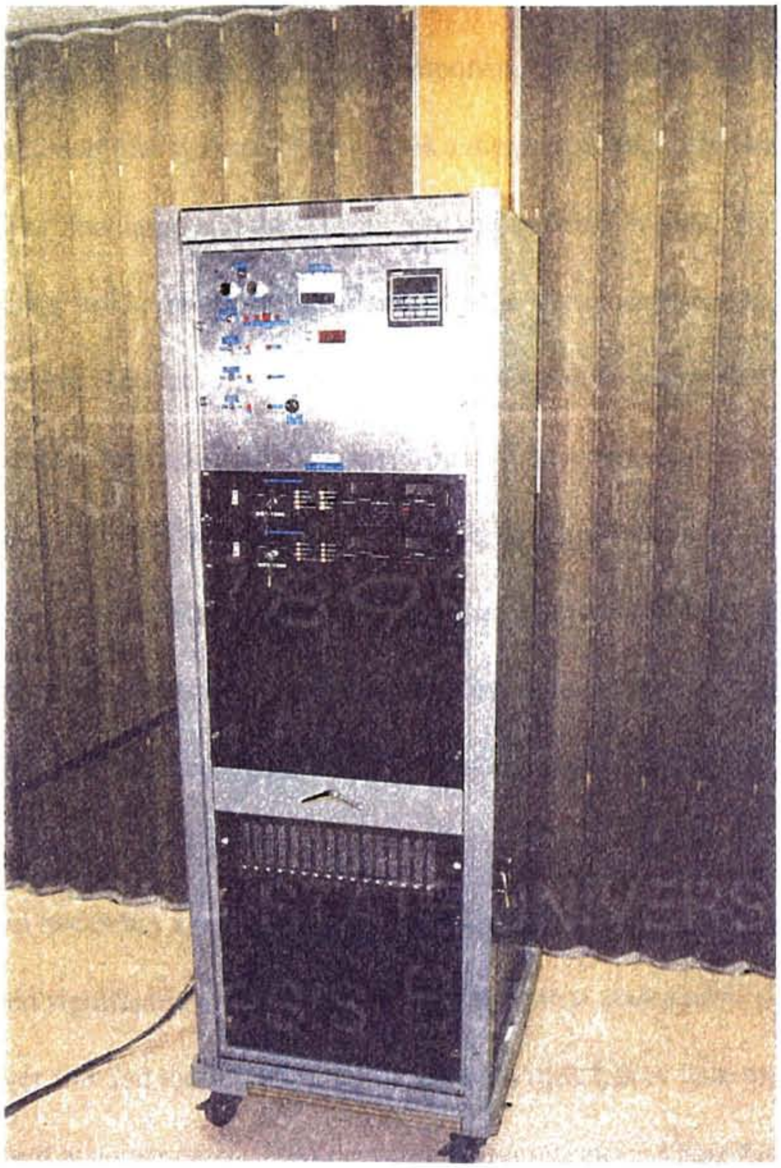

Figure 11

Operational Flashlamp Pumped Laser Power Supply/Controller

CHAPTER III

LASER HEAD

The laser head is made up of several components which allow the device to pump the gain media and cool the system. Figure 12 is a diagram of the laser head configuration. The flashlamp and the Alexandrite rod are held in place via a sapphire holder. The circular holder holds the flashlamp and the Alexandrite rod in a closely coupled arrangement. This ensures that the flashlamp is able to pump the Alexandrite rod reasonably uniformly from all sides. The sapphire holder is surrounded by polished silver foil which acts as a reflector for the pump light pulse. For low temperature applications, there is a thin film of thermal compound on the outside of the silver foil which provides adequate thermal contact between the sapphire assembly and the aluminum cooling fins between which it is sandwiched. However, for high temperature operation, the thermal compound was replaced with .004 inch thick aluminum foil. This modification was necessary since at the higher temperatures the thermal compound's viscosity dropped significantly which allowed it to flow into undesirable areas, i.e. between the silver foil and the sapphire holder where it then baked onto these surfaces. The system is kept at a user defined temperature via temperature controller and fans. The temperature controller determines the laser head temperature using a thermocouple attached to the cooling fin assembly and increases or decreases the air flow from the fans accordingly.

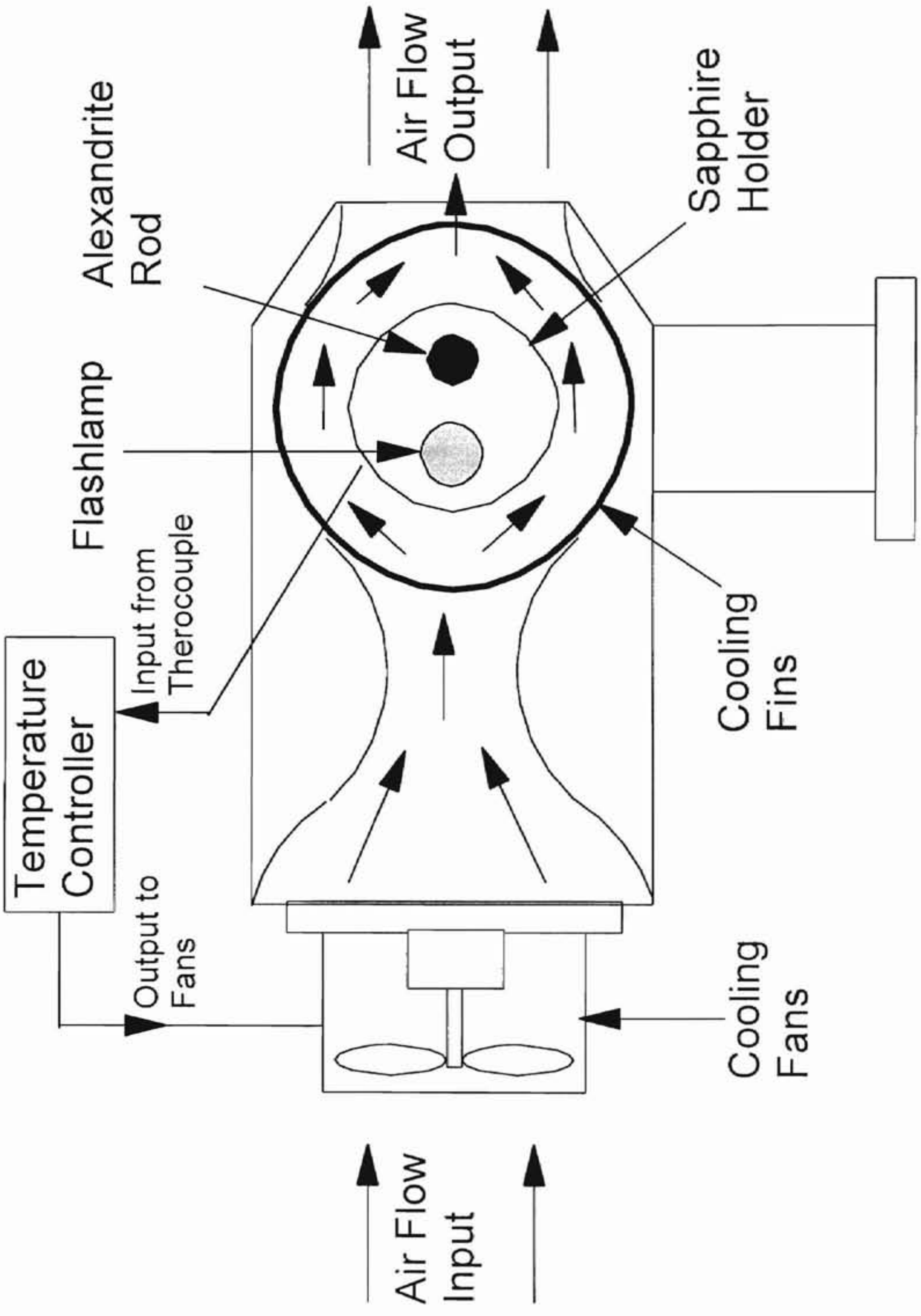

Figure 12

Laser Head Diagram.

CHAPTER IV

LASER CHARACTERIZATION

Free Running Alexandrite Laser

Experimental Setup

The cavity used for the free running laser characterization tests is set up in a standing-wave configuration for both the 10% and 20% outcoupled cavities. Figure 13 is a diagram of the experimental setup as well as the cavity layout. The cavity consists of the gain medium (Alexandrite rod), 0° high reflective mirror, output coupler (10% or 20%), 45° high reflective mirror, and a two element birefringent tuner.

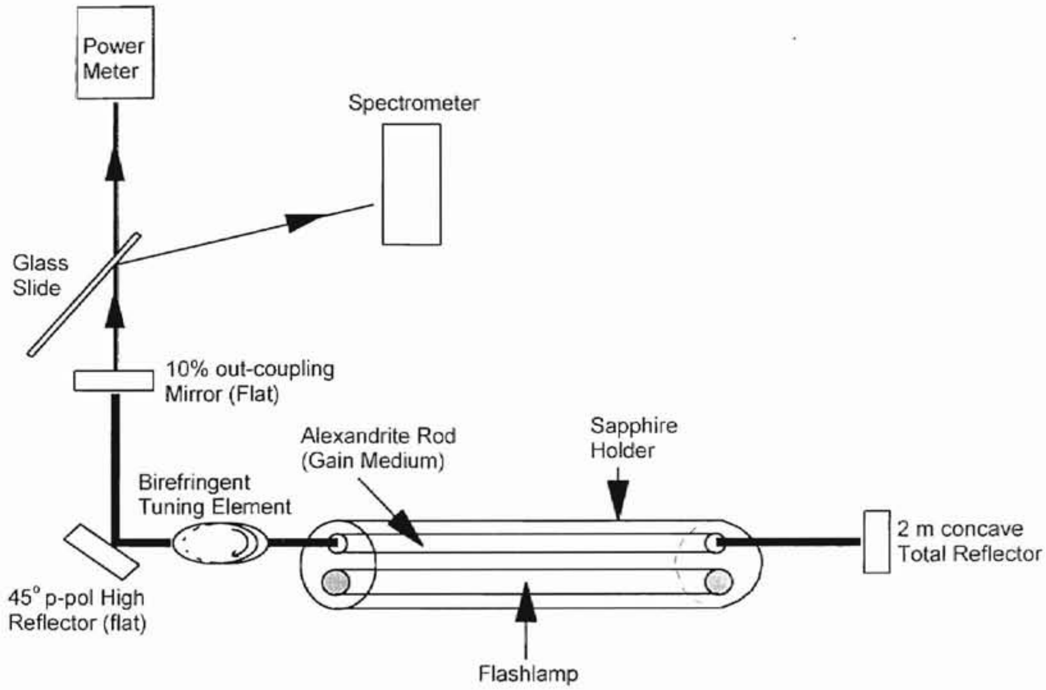

Figure 13

Free-Running Flashlamp Pumped Alexandrite Laser Cavity.

10% Outcoupled Cavity Characteristics

Figure 14 shows the tunable wavelength range of the 10% outcoupled laser with respect to temperature. The plot shows that the optimum temperature for maximum operational range is between 90 °C and 130 °C. The maximum output power and threshold voltage with respect to temperature are given in Figure 15. Maximum output power was obtained at 100 °C which is conveniently within the range of the maximum tunability regime. Figure 16 shows the minimum and maximum lasing wavelengths as well as the maximum output power wavelengths with respect to temperature. This plot reveals that the minimum lasing wavelengths, maximum lasing wavelengths, and maximum output power wavelengths all increase as the cavity temperature rises.

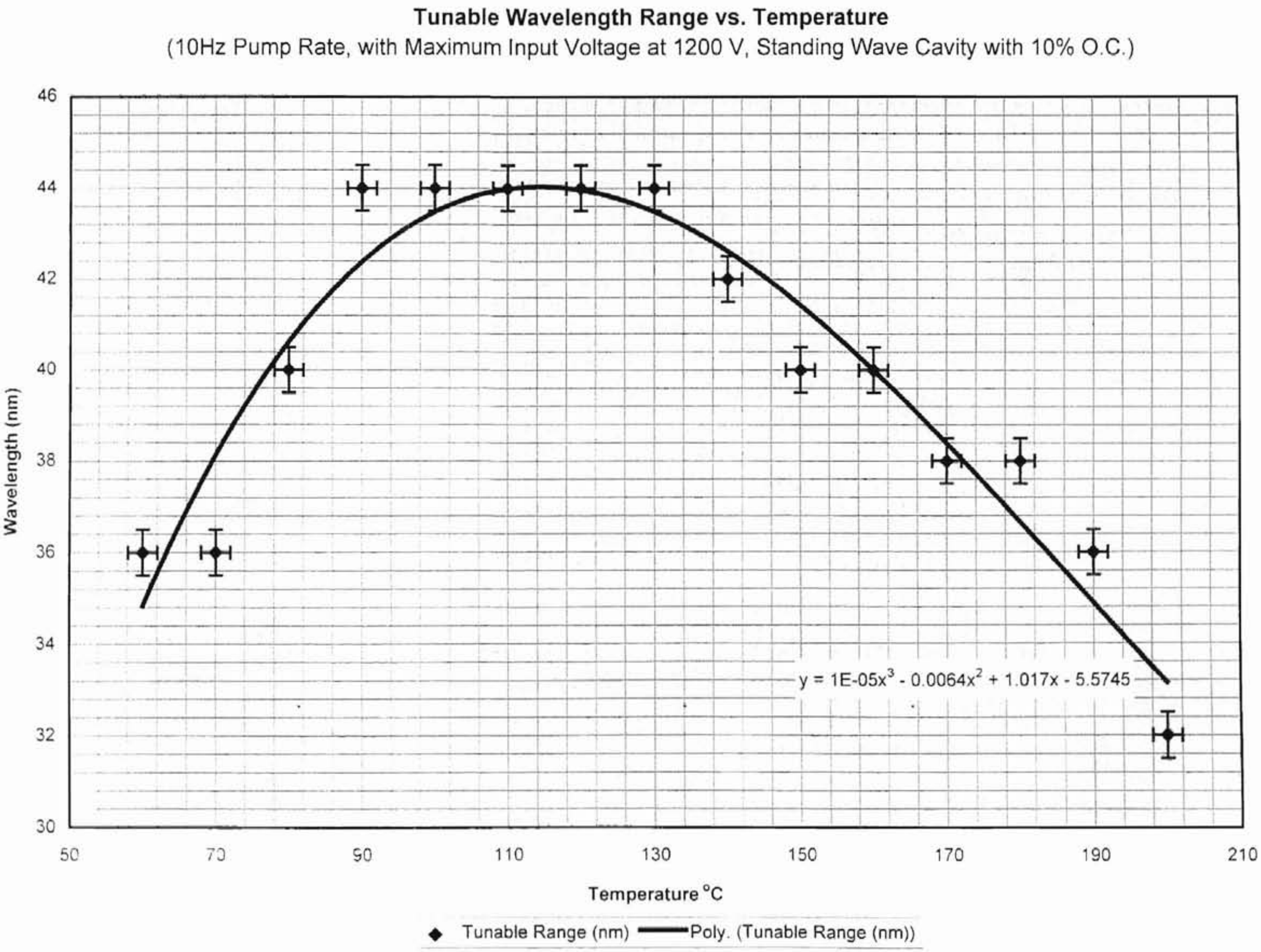

Figure 14

Tunable Wavelength Range vs. Temperature for the 10% Outcoupled Alexandrite Laser.

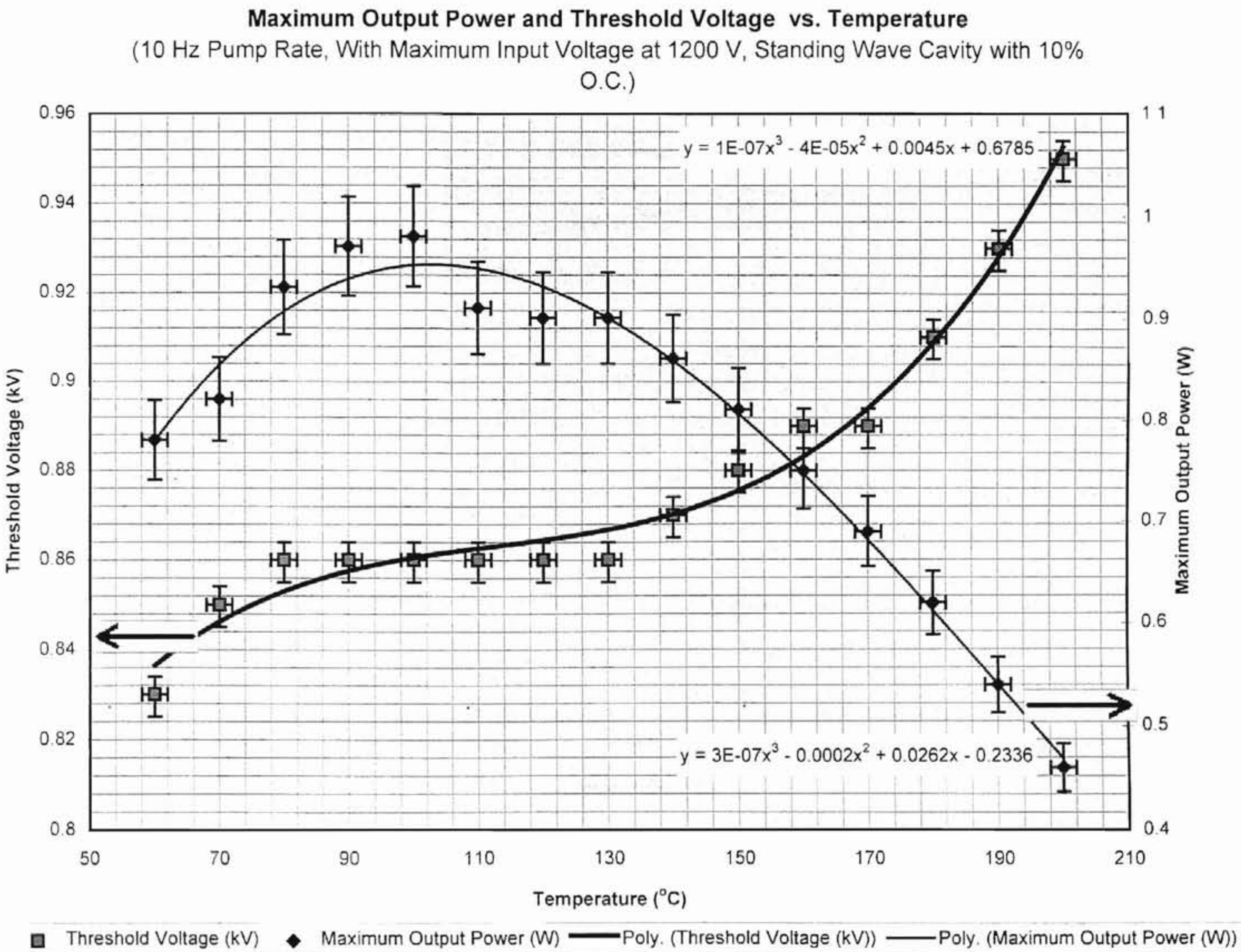

Figure 15

Maximum Output Power and Threshold Voltage vs. Temperature for the 10% Outcoupled Alexandrite Laser.

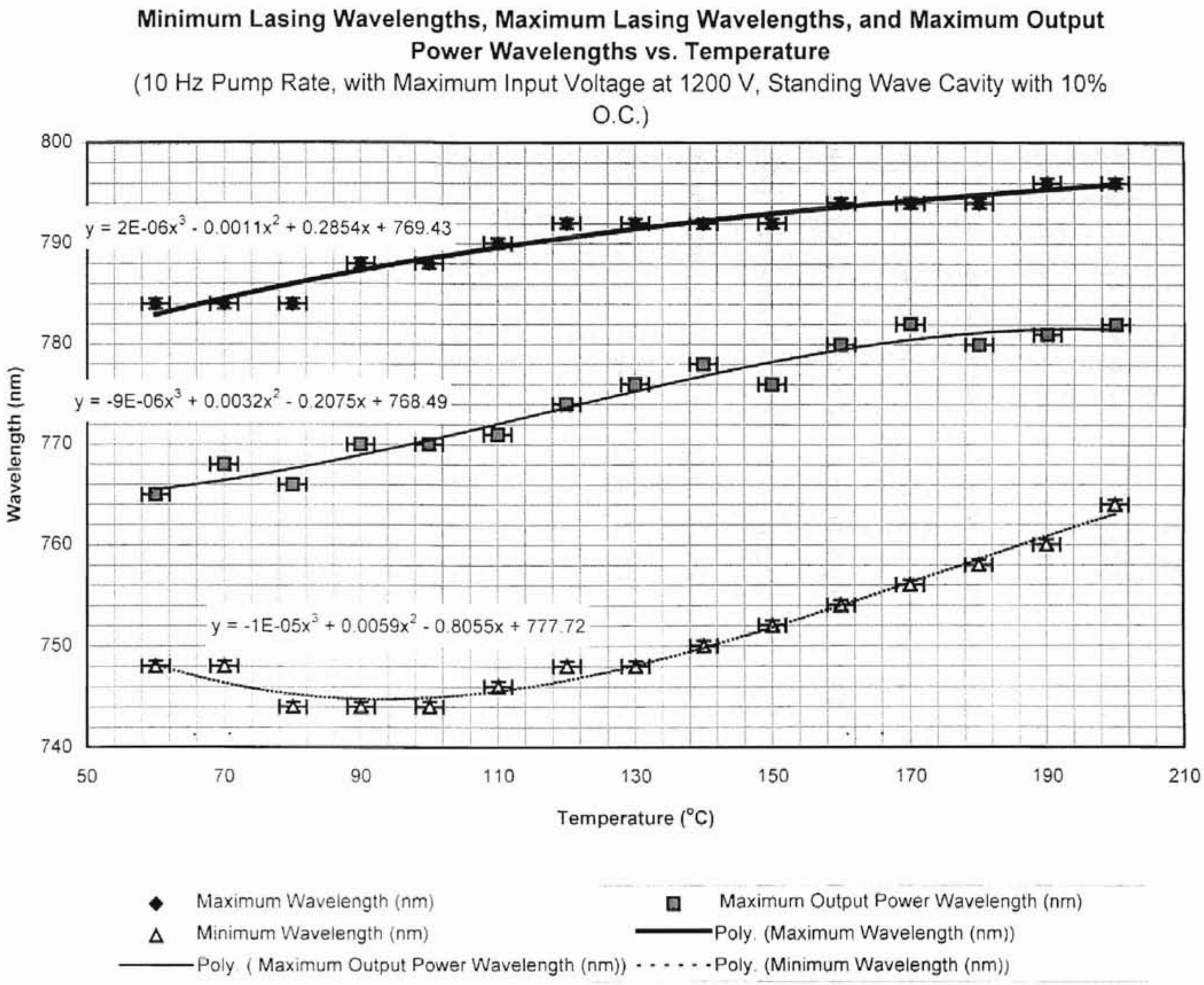

Figure 16

Minimum Lasing Wavelengths, Maximum Lasing Wavelengths and Maximum Output Power Wavelengths vs. Temperature for the 10% Outcoupled Alexandrite Laser.

20% Outcoupled Cavity Characteristics

Figure 17 shows the tunable wavelength range of the 20% outcoupled laser with respect to temperature. The plot shows that the optimum temperature for maximum operational range is between 90 °C and approximately 120 °C. Figure 18 depicts the maximum output power and threshold voltage with respect to temperature. Maximum output power was obtained at 100 °C, which is also in the area of the maximum tunability range. The minimum and maximum lasing wavelengths as well as the maximum output power wavelengths with respect to temperature are indicated in Figure 19. This plot also reveals that the minimum lasing wavelengths, maximum lasing wavelengths, and maximum output power wavelengths all increase as the cavity temperature increases.

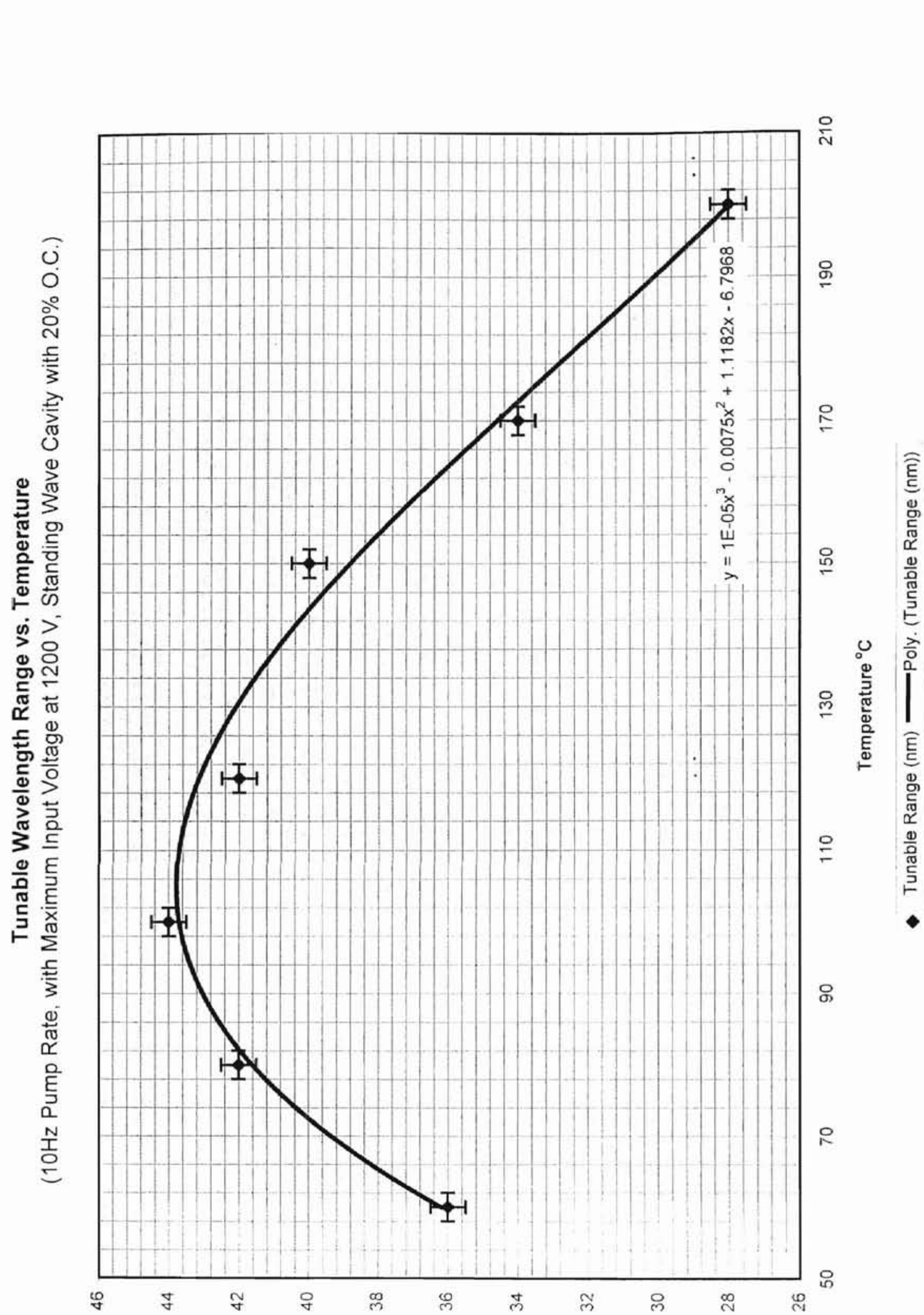

Figure 17

Tunable Wavelength Range vs. Temperature for the 20% Outcoupled Alexandrite Laser.

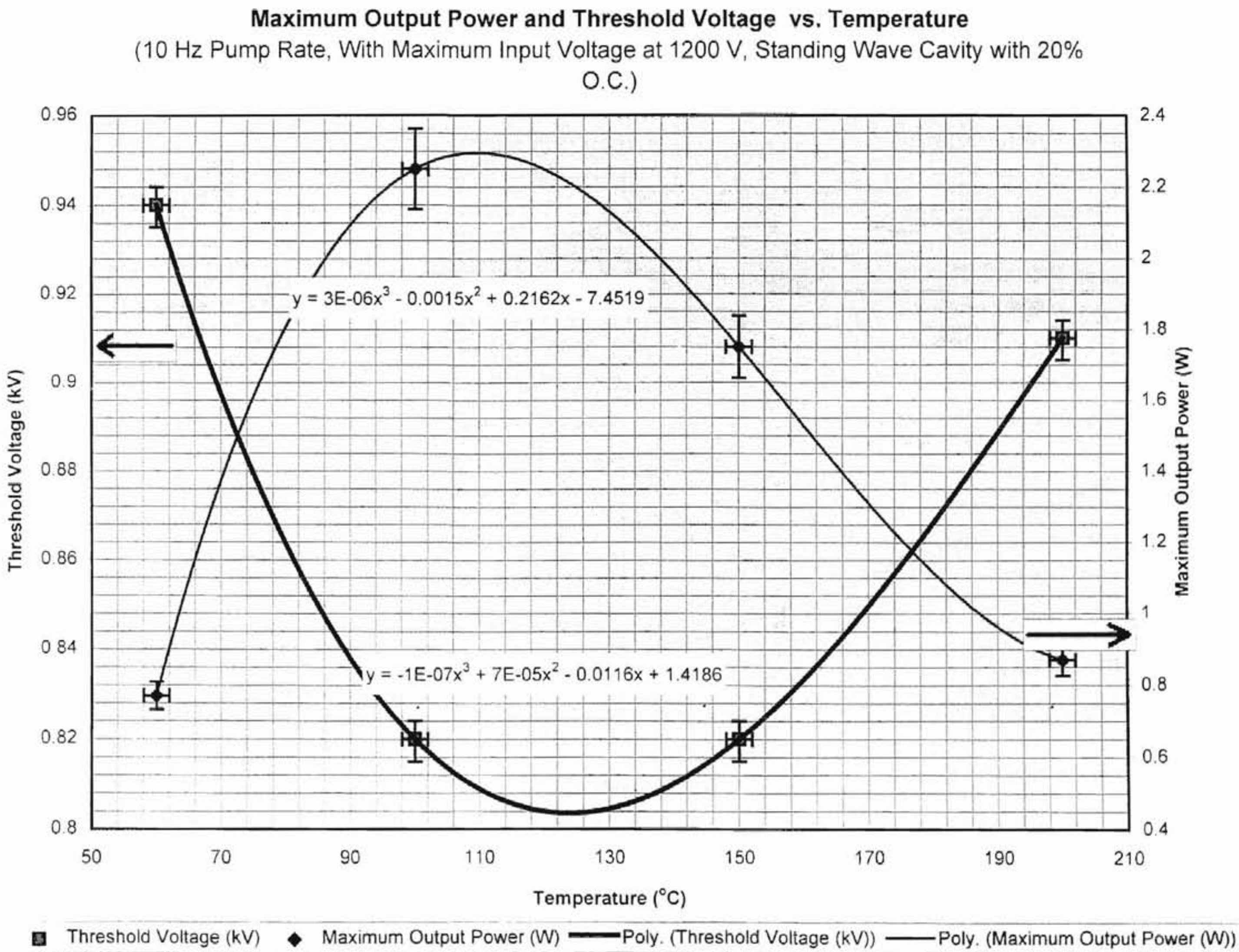

Figure 18

Maximum Output Power and Threshold Voltage vs. Temperature for the 20% Outcoupled Alexandrite Laser.

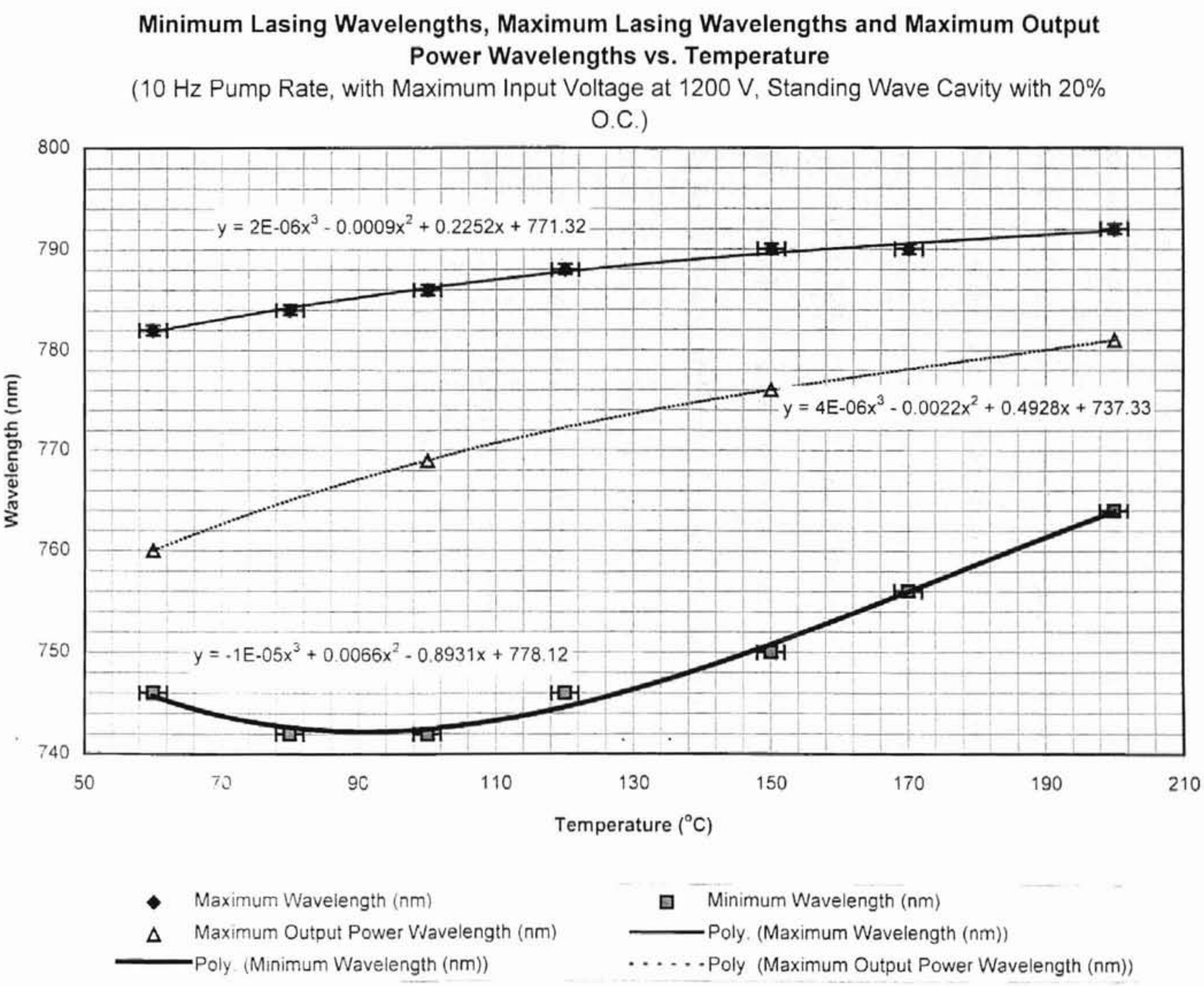

Figure 19

Minimum Lasing Wavelengths, Maximum Lasing Wavelengths and Maximum Output Power Wavelengths vs. Temperature for the 20% Outcoupled Alexandritic Laser.

10% and 20% Outcoupled Laser Comparisons

The comparisons of the tunable wavelength ranges for both the 10% and 20% outcoupled lasers with respect to temperature are given in Figure 20. This shows that the two cavities have similar operational ranges with respect to temperature. Figure 21 shows the comparisons of the output power and threshold voltage with respect to temperature range at 770 nm for both the 10% and 20% outcoupled lasers. This plot reveals that the 20% outcoupled cavity has more than double the output power of the 10% outcoupled cavity. The minimum and maximum lasing wavelengths as well as the maximum output power wavelengths with respect to temperature range for both the 10% and 20% outcoupled lasers are depicted in Figure 22. The diagram also indicates that the two cavities have similar obtainable wavelengths with respect to temperature. This information shows that both the 10% and 20% outcoupled cavities have similar characteristics except that the 20% outcoupled cavity is capable of much higher output power.

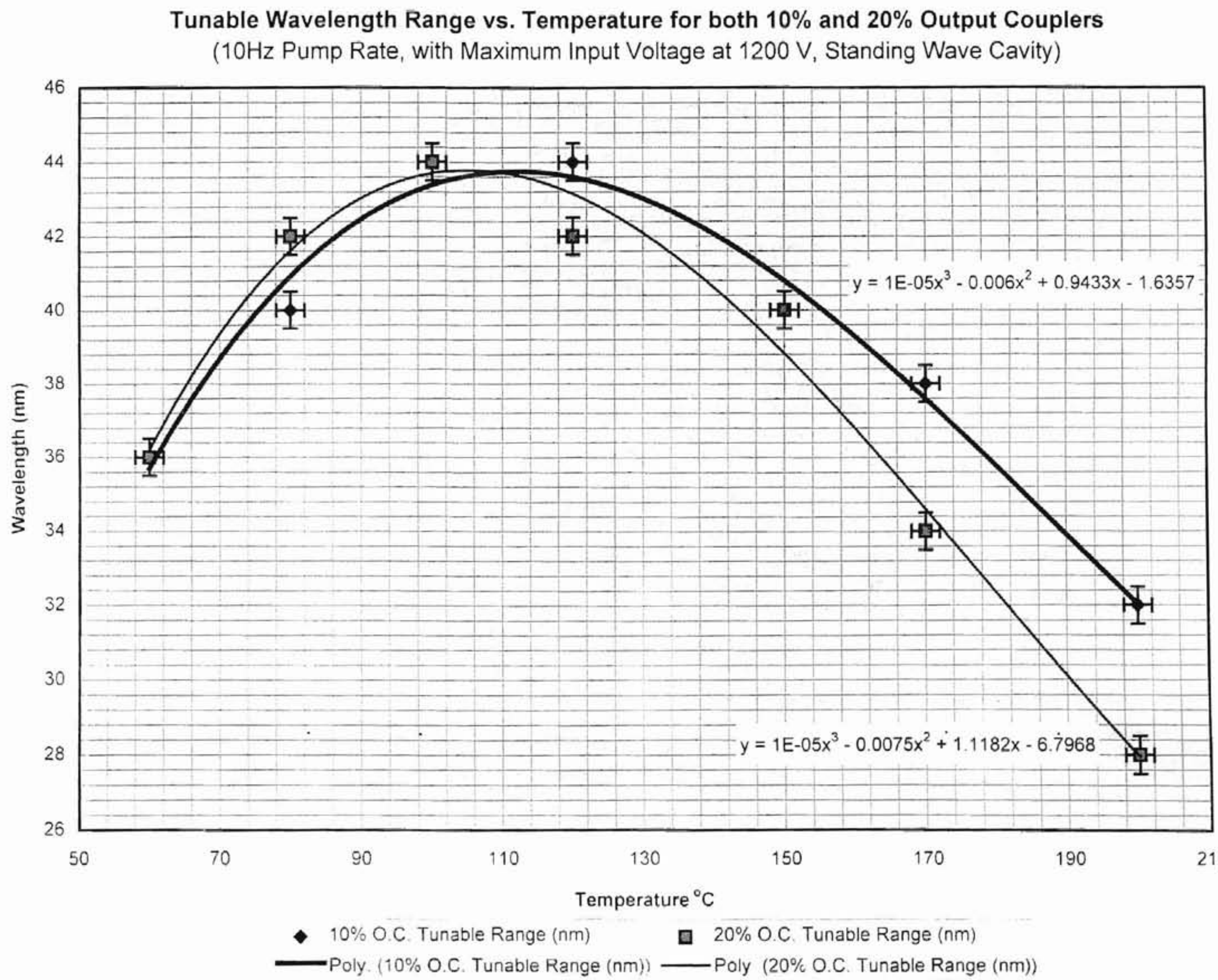

Figure 20

Tunable Wavelength Range vs. Temperature for Both 10% and 20% Outcoupled Laser Cavities.

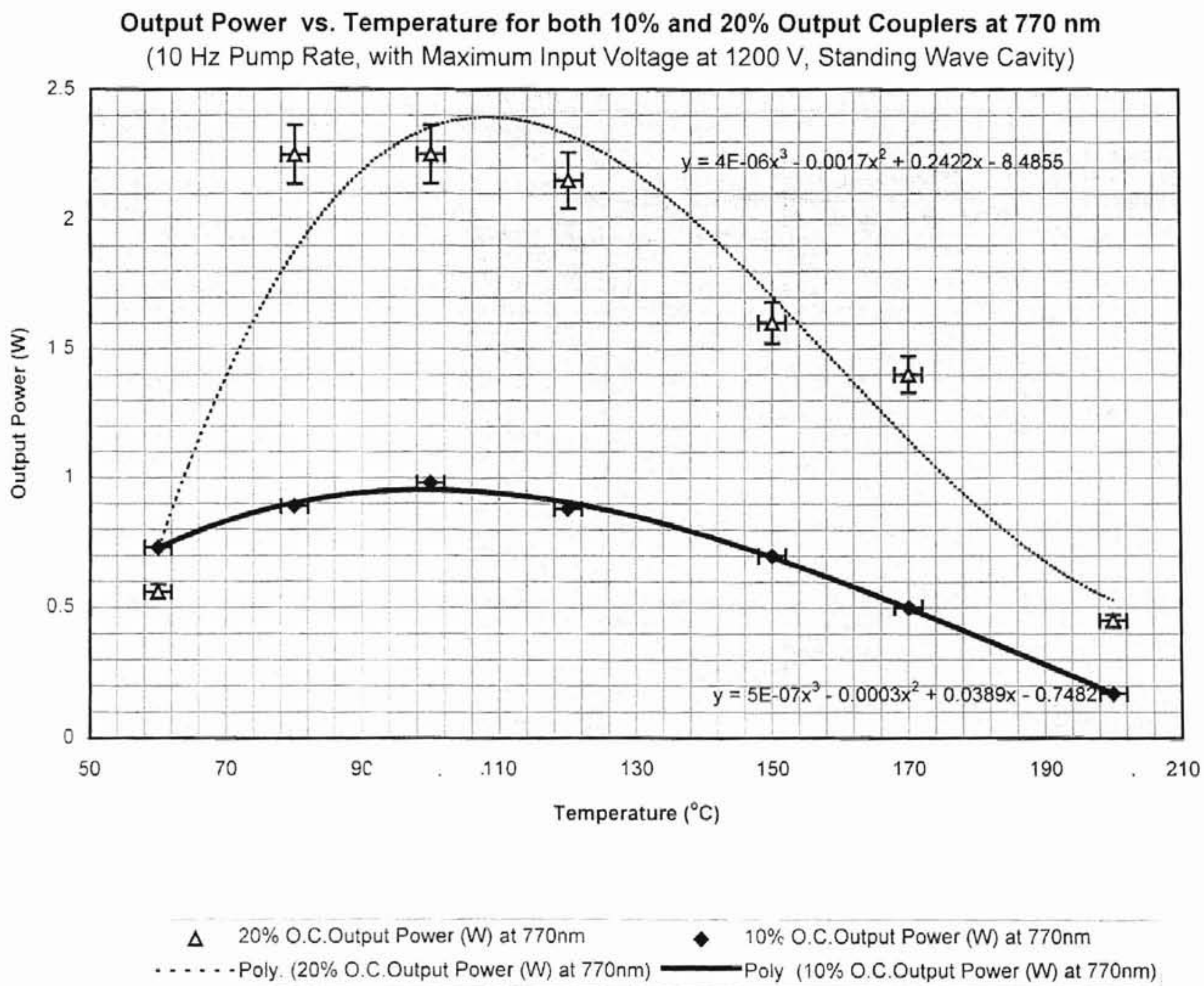

Figure 21

Output Power and vs. Temperature at 770 nm for Both 10% and 20% Outcoupled Laser Cavities.

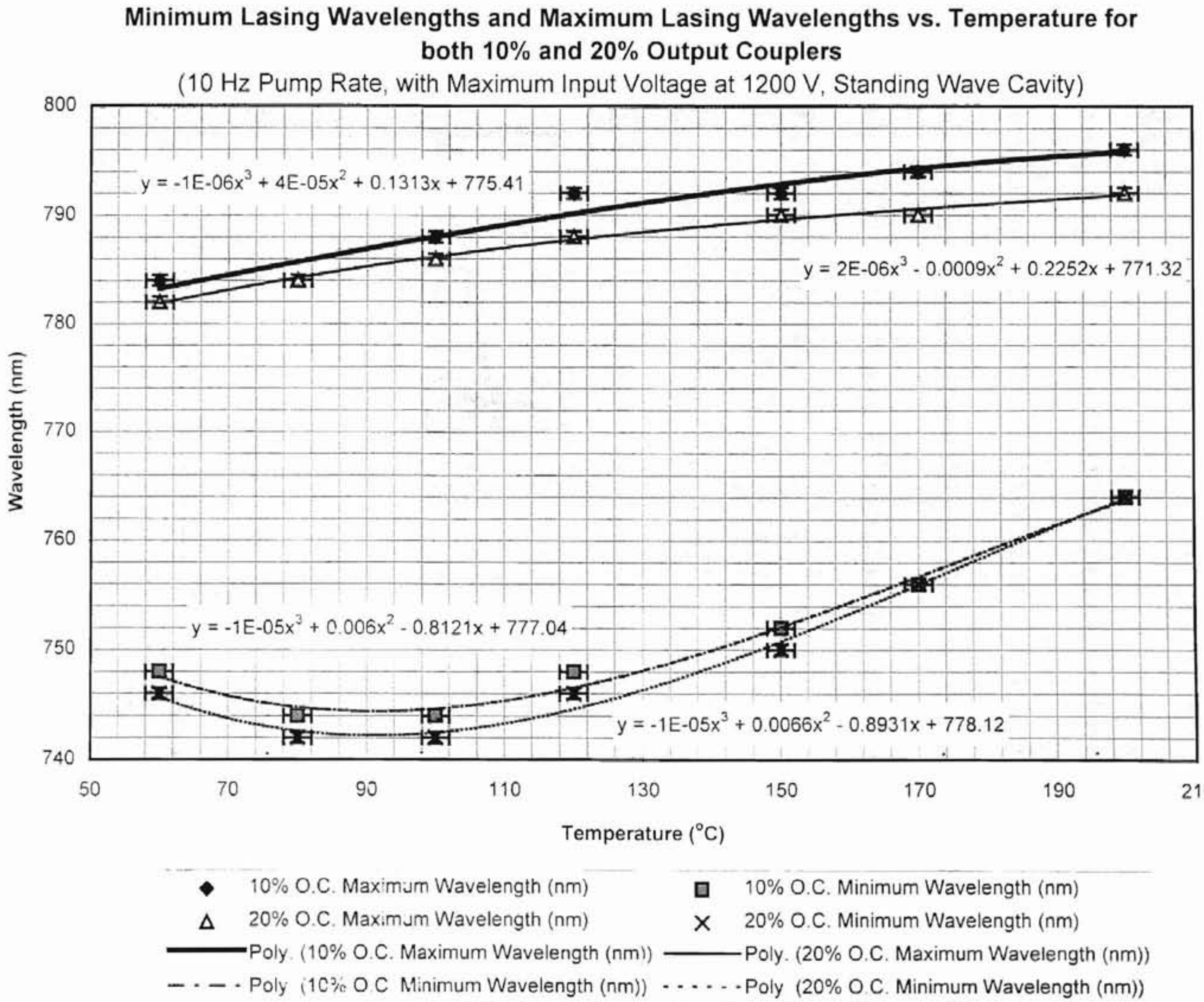

Figure 22

Minimum Lasing Wavelengths and Maximum Lasing Wavelengths vs. Temperature for Both 10% and 20% Outcoupled Laser Cavities.

Q-SWITCHED LASER

Experimental Setup

The cavity used for the Q-switched laser characterization tests is set up in a standing wave configuration. Figure 23 is a diagram of the experimental setup as well as the cavity layout. The cavity consists of the gain medium (Alexandrite rod), 0° high reflective mirror, 50% output coupler, 45° high reflective mirror, a two element birefringent tuner and a Q-switch.

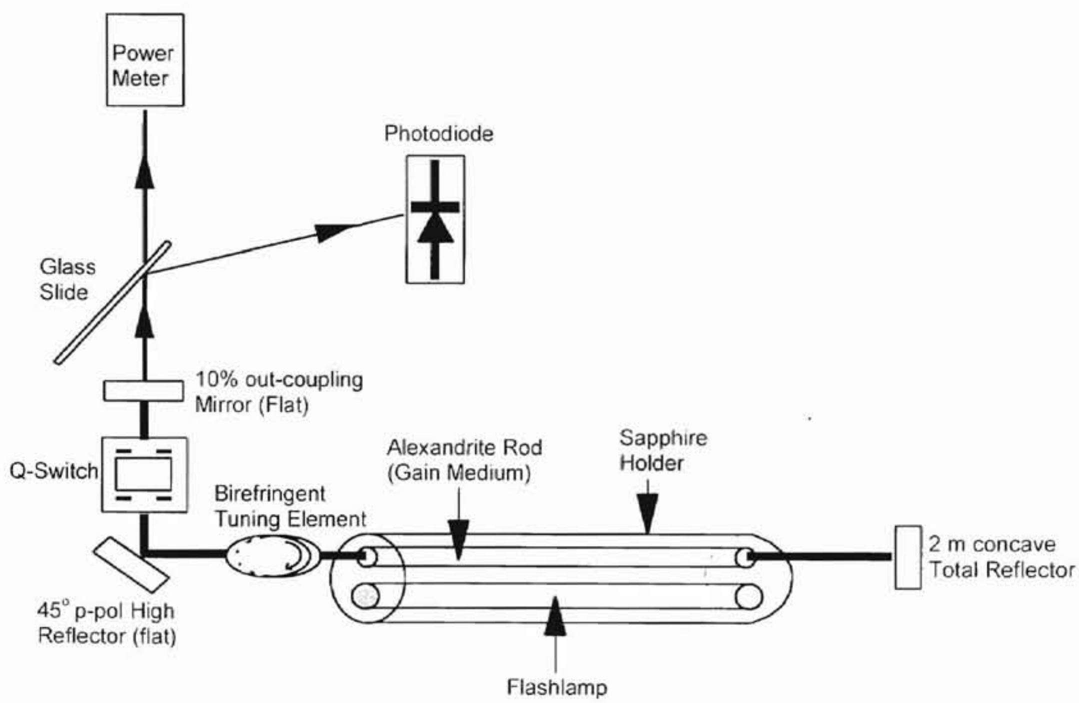

Figure 23

Q-Switched Flashlamp Pumped Alexandrite Laser Cavity.

Q-Switch Driver

The main components of the Q-switch driver are a hydrogen krytron, two to one transformer, transistor module, 1 kV and 10 kV power supplies. The hydrogen krytron, produced by EG&G, is a high voltage/current device. It has a very short rise time and is capable of switching large amounts of current. The transistor module is a fast power mosfet capable of rise times of only a few nanoseconds and was obtained from Directed Energy, Incorporated. The laser cavity is prevented from lasing by applying the proper $\lambda/4$ voltage across the pockels cell thereby introducing a $\lambda/2$ delay in the cavity. This delay causes the cavity to have a low quality factor and therefore prevents lasing. The Q-switch driver receives a delayed trigger pulse from the power supply/controller to the transistor module, which in turn triggers the hydrogen krytron. When the hydrogen krytron is triggered, the 2.42 kV ($\lambda/4$ voltage) across the pockels cell is dropped to approximately 0 V. The quality factor of the cavity increases thus allowing the laser cavity to lase. Once current stops flowing through the krytron, the krytron opens and the $\lambda/4$ voltage is restored across the pockels and the cavity's quality factor is once again low, preventing lasing until the next trigger pulse.

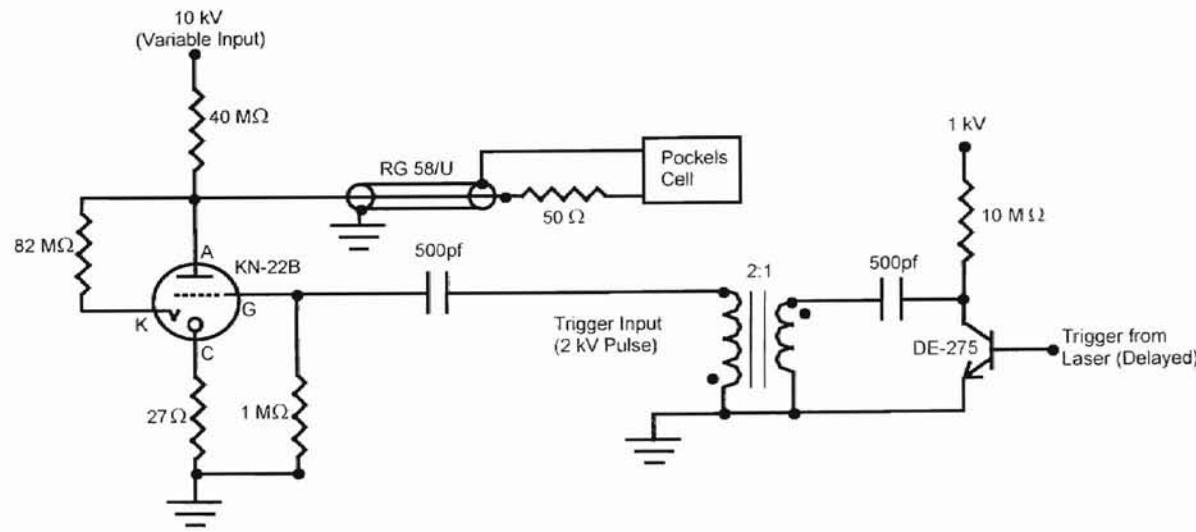

Figure 24

Q-Switch Driver Circuit.

Q-Switched Cavity Characteristics

Figure 25 shows the output pulse of the laser with no Q-switch. The free running pulse of the laser actually consists of multiple pulses with the pulse envelope approximately 27 μs long. Figure 26 shows the output pulse of the laser with the Q-switch driver set at the λ/4 voltage, but multiple pulses still exist due to the trigger pulse delay being of an insufficient value. This gives a pulse envelope of approximately 17 μs which is almost half the length of the long pulse and will continue to decrease in length until the proper trigger delay is obtained. Figure 27 shows the output pulse of the laser with the proper trigger delay of the Q-switch set at 90 μs. The output pulse is a single pulse and the amplitude is an order of magnitude greater than the output pulse with no Q-switch. The Q-switched pulse width is only 150 ns at FWHM. Therefore, the Q-switched pulse has all the energy in one high intensity short pulse. These pulse characteristics are necessary if the laser is to be used for second and third harmonic generation to increase the usable frequency range. This would be necessary in order to implement the laser as a LiDAR system. Figure 28 shows the pulse amplitude and pulse length vs. Q-switch trigger delay for the laser. A photograph of the actual flashlamp pumped laser cavity is depicted in Figure 29. As the trigger delay is increased past the optimum 90 μs delay, the pulse amplitude decreases and the pulse width increases until finally the laser will no longer lase.

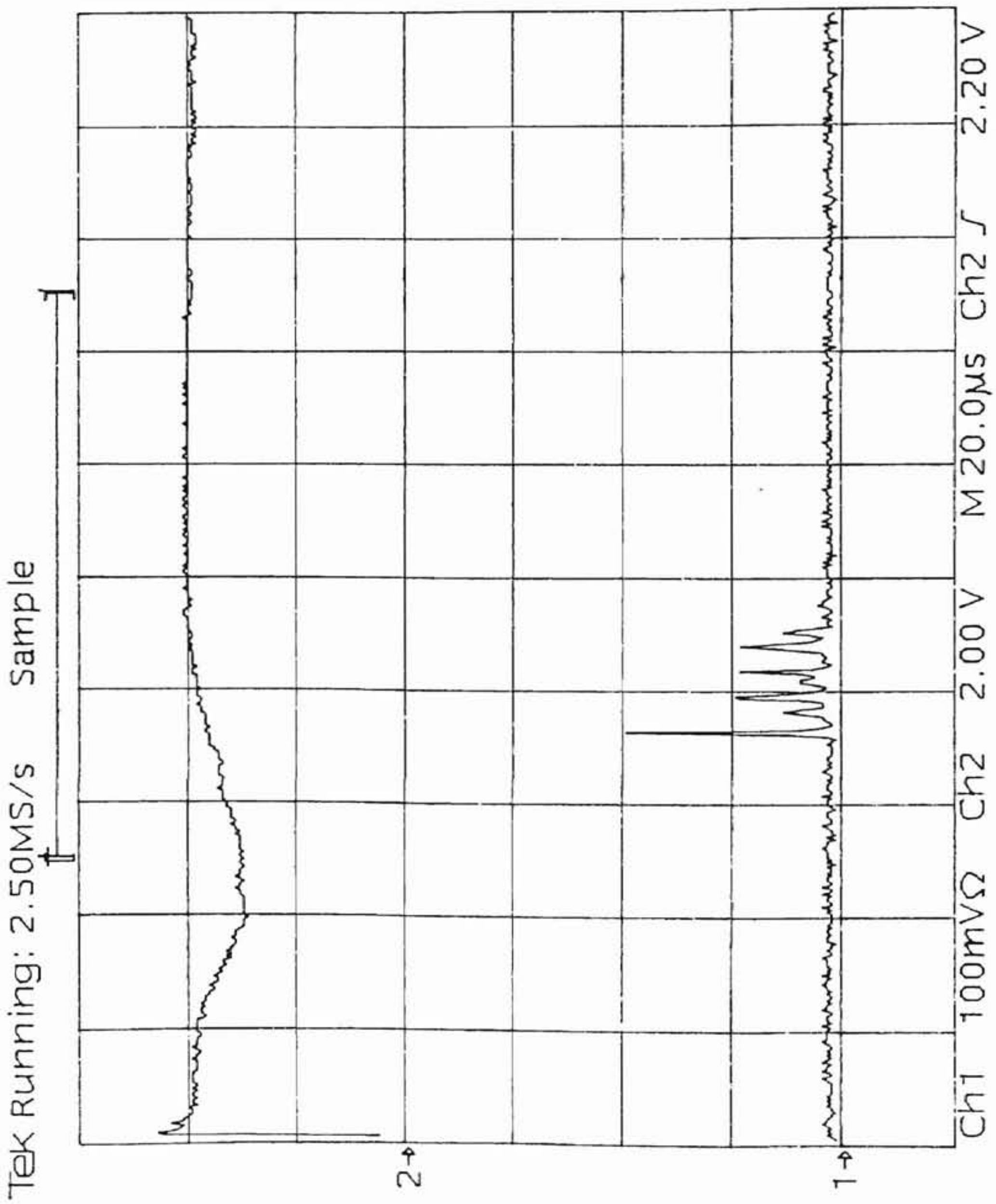

Figure 25

Output Pulse of Alexandrite Laser with No Q-Switch.

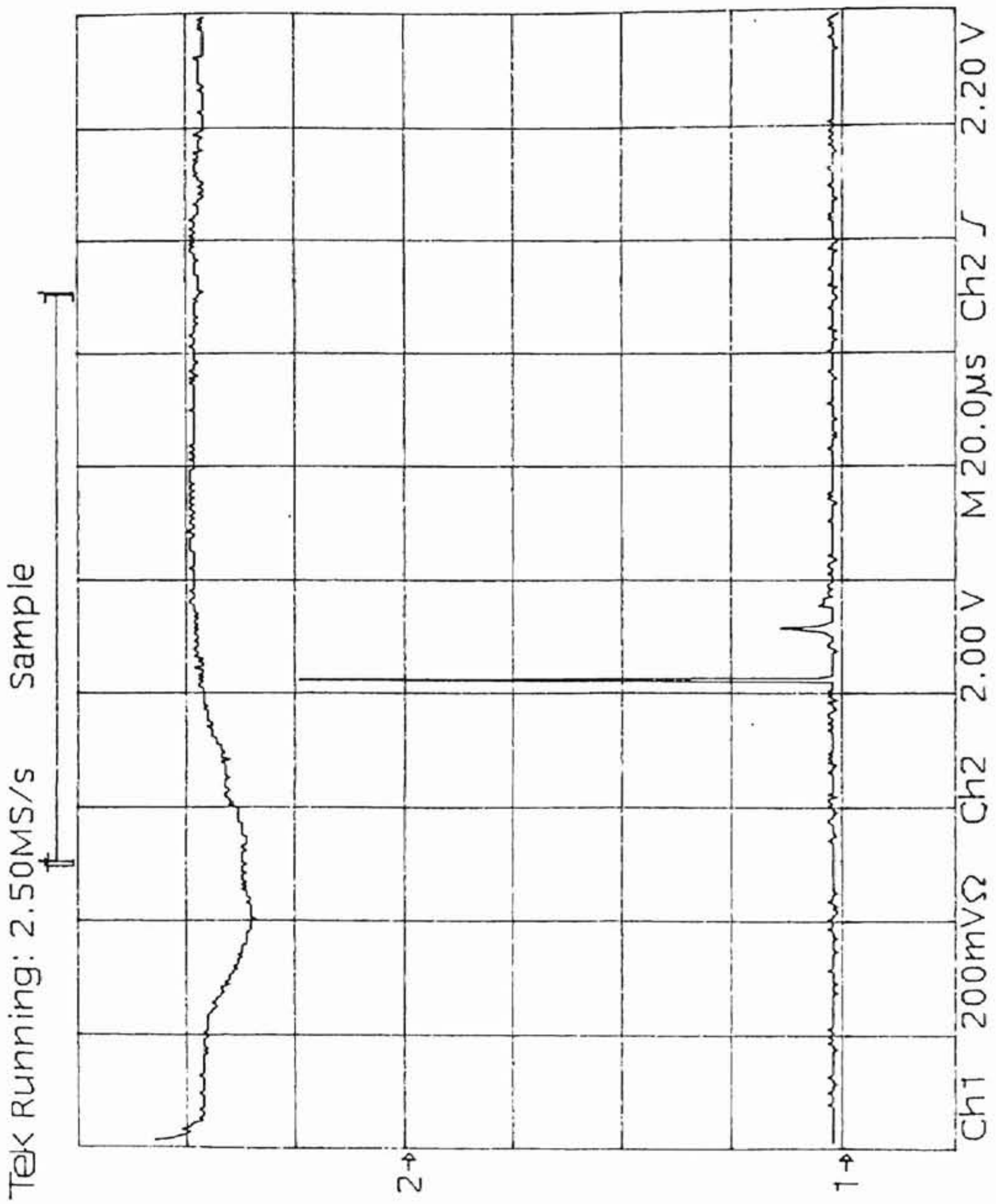

Figure 26

Output Pulse of Q-Switched Laser with 80 μs Delay.

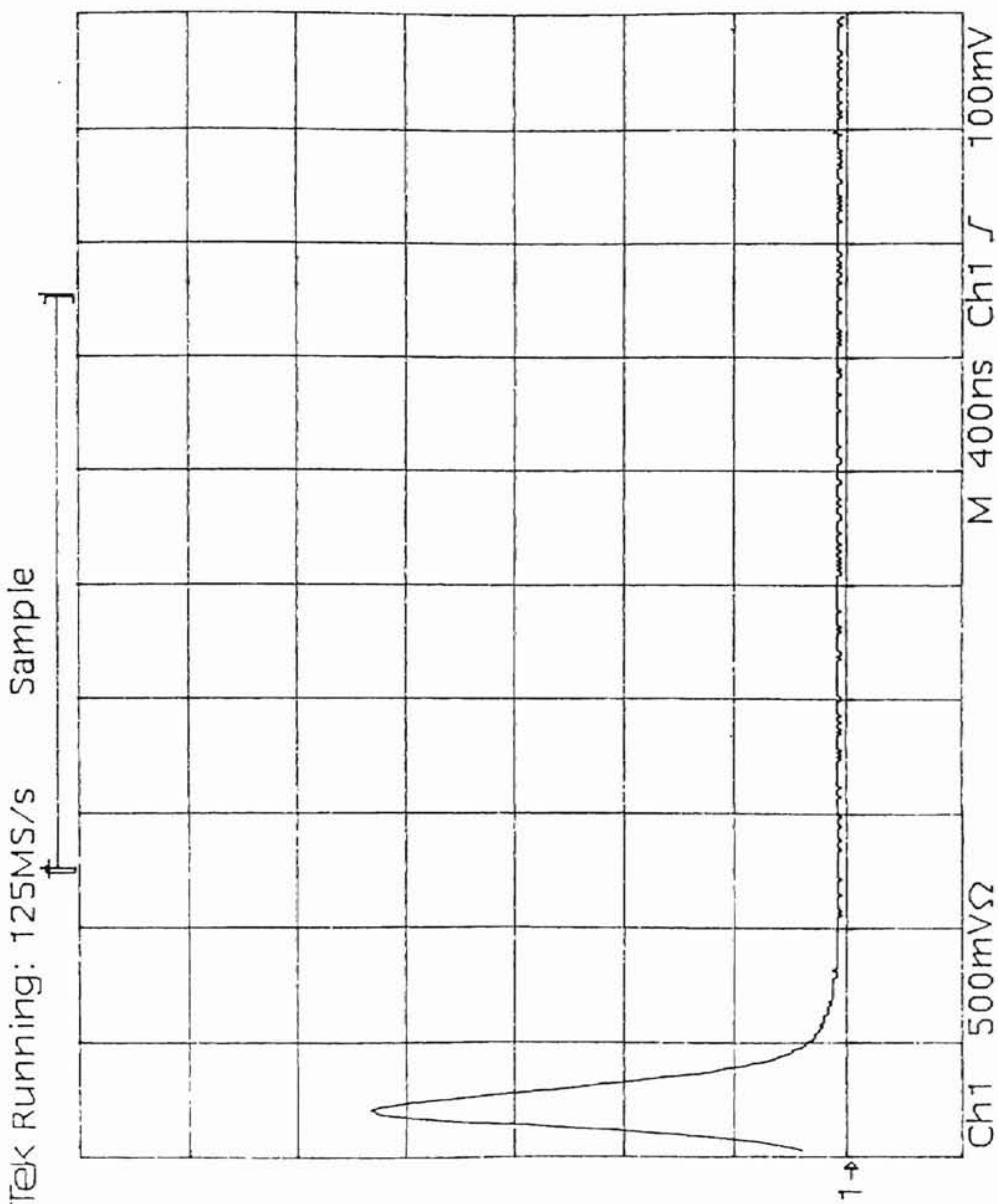

Figure 27

Output Pulse of Q-Switched Laser with 90 μs Delay.

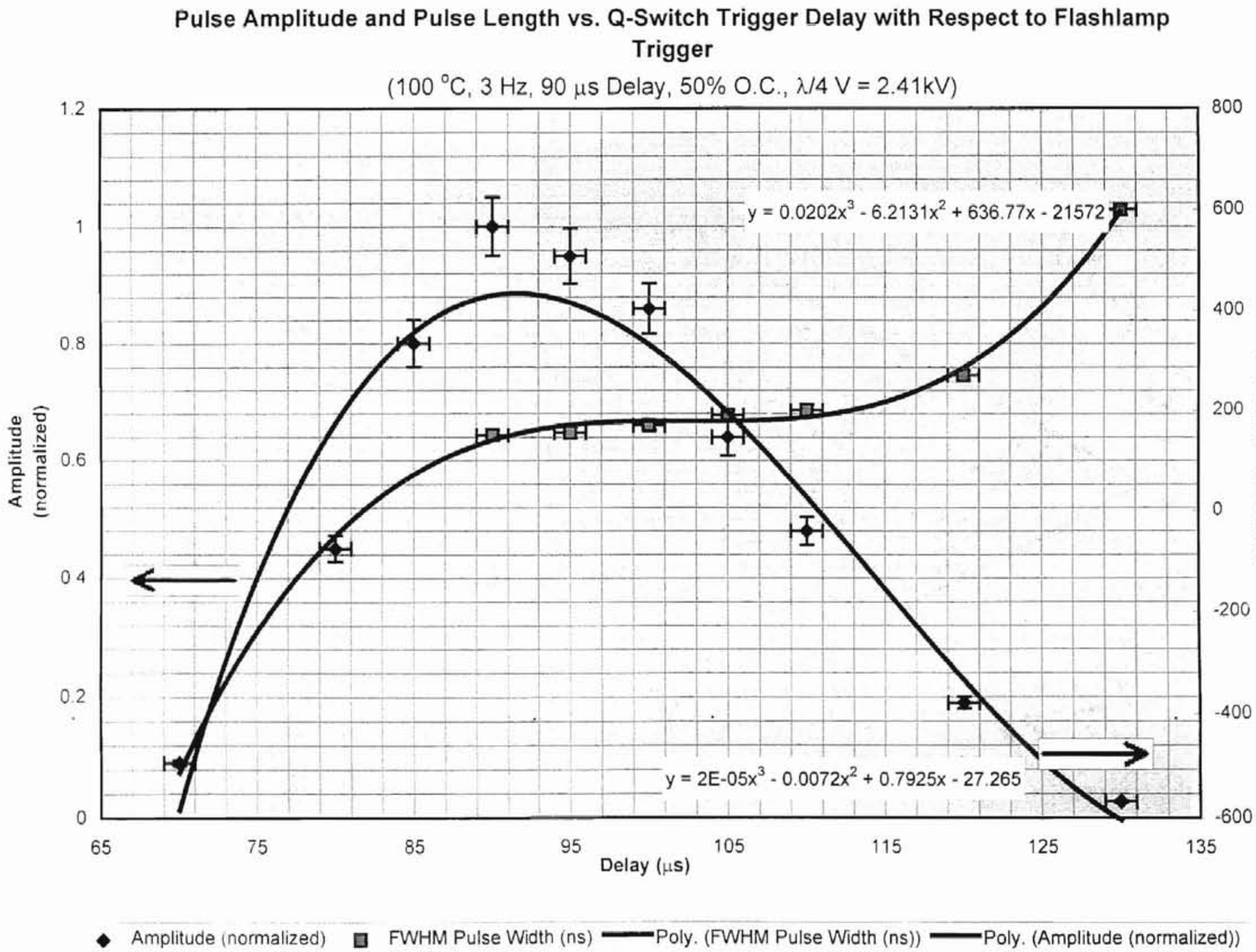

Figure 28

Pulse Amplitude and Pulse Length vs. Q-Switch Trigger Delay.

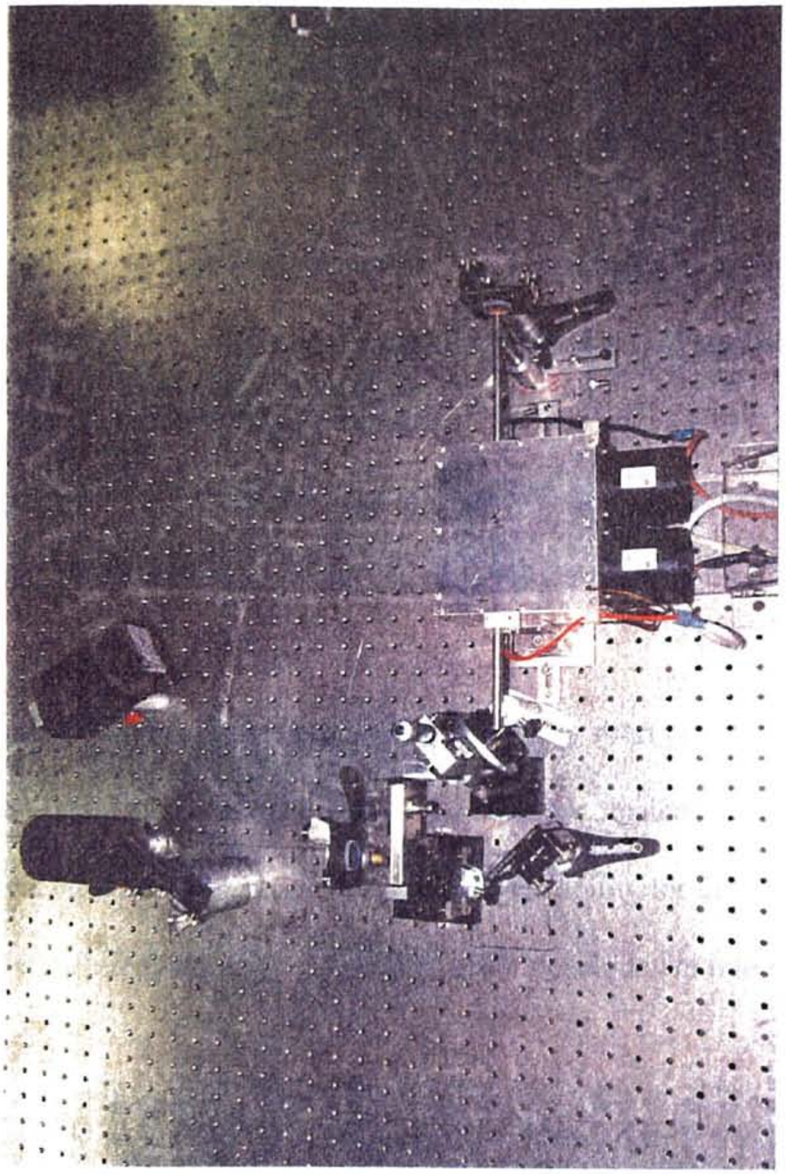

Figure 29

Operational Flashlamp Pumped Laser

CHAPTER V.

SUMMARY, CONCLUSIONS, RECOMMENDATIONS

The output wavelength of the flashlamp pumped Alexandrite laser was tunable from 740 nm to 796 nm in a temperature range of 60 °C and 200 °C and at a pump energy of 36 J/pulse. The maximum output power under these conditions was 2.25 Watts at a 10 Hz repetition rate which corresponds to 225 mJ/pulse. In Q-switched operation, the laser was also tunable and capable of producing large amplitude 150 ns pulses.

The capability of the laser to produce high intensity short pulses makes it possible to use second and third harmonic generation to increase the obtainable frequency range of the laser. The fact that the laser is air-cooled implies the ability for the laser to be portable, and with a large frequency range, capable for development into a LiDAR system.

For continued development of the LiDAR system, it will be necessary to experiment with both intra- and extra-cavity second and third harmonic generation. This experimentation should be tested in both standing wave and ring laser configurations to determine the power output across the wide frequency range of the laser.

Miniaturization of the power supply and complete laser cavity will also need to be provided to enable the laser to become a portable size and therefore viable as a LiDAR system.

REFRENCES

1. Demtröder, Wolfgang. Laser Spectroscopy Basic Concepts and Instrumentation. 2nd ed. New York, NY: Springer-Verlag, 1996.

2. Walling, John C., Otis, PetersonG., Jenssen, Hans P., Morris, Robert C. and O'Dell, E. Wayne. Tunable Alexandrite Lasers. IEEE Journal of Quantum Electronics, Vol. Qe-16, No. 12, Dec. 1980.

3. Koechner, Walter. Solid-State Laser Engineering. 3rd ed. New York, NY: Springer-Verlag, 1992.

4. Allied Signal Corporation. New Jersy. Technical Briefs.

APPENDIX A

PARTS LIST

D1. NTD-20, 20 kV Diode from EDI

D2. VC-40, 4 kV Diodes from Micro Quality Semiconductor, Inc.

D3. VC-40, 4 kV Diodes from Micro Quality Semiconductor, Inc.

D4. VC-120, 12 kV Diodes from Micro Quality Semiconductor, Inc.

D5. VC-120, 12 kV Diodes from Micro Quality Semiconductor, Inc.

D6. SKR 130/16 HV Diode from Semikron, Inc.

SCR1/SCR2. Semipack SKKT 72/20E from Semikron, Inc.

DE-275. 275FPS-1N from Directed Energy, Inc.

KN-22B. Hydrogen Krytron from EG&G, Inc.

APPENDIX B

TTL LOGIC FLOW DIAGRAM

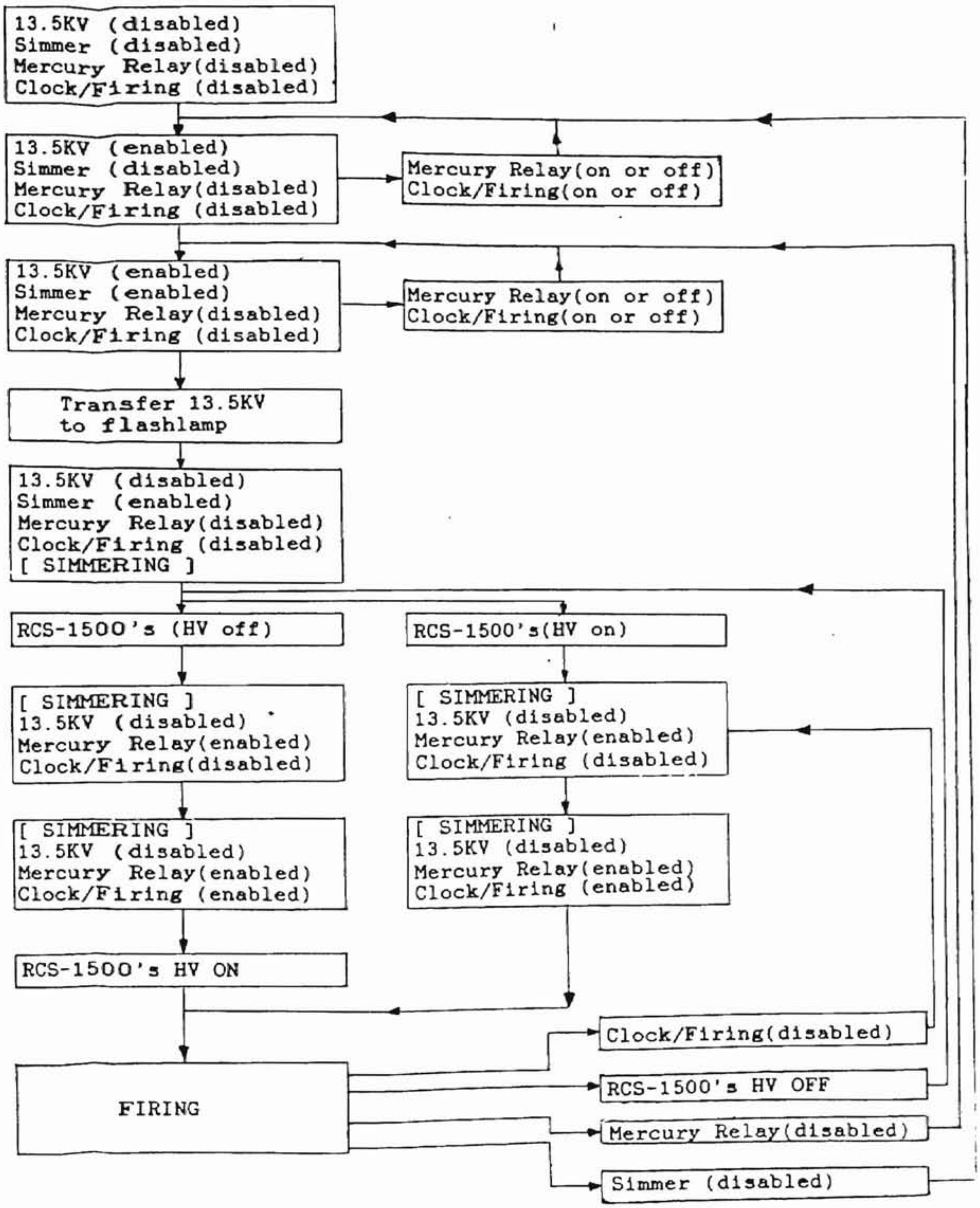

Figure 30

TTL Logic Flow Diagram.

APPENDIX C

FLASHLAMP OUTPUT PULSE DIAGRAMS

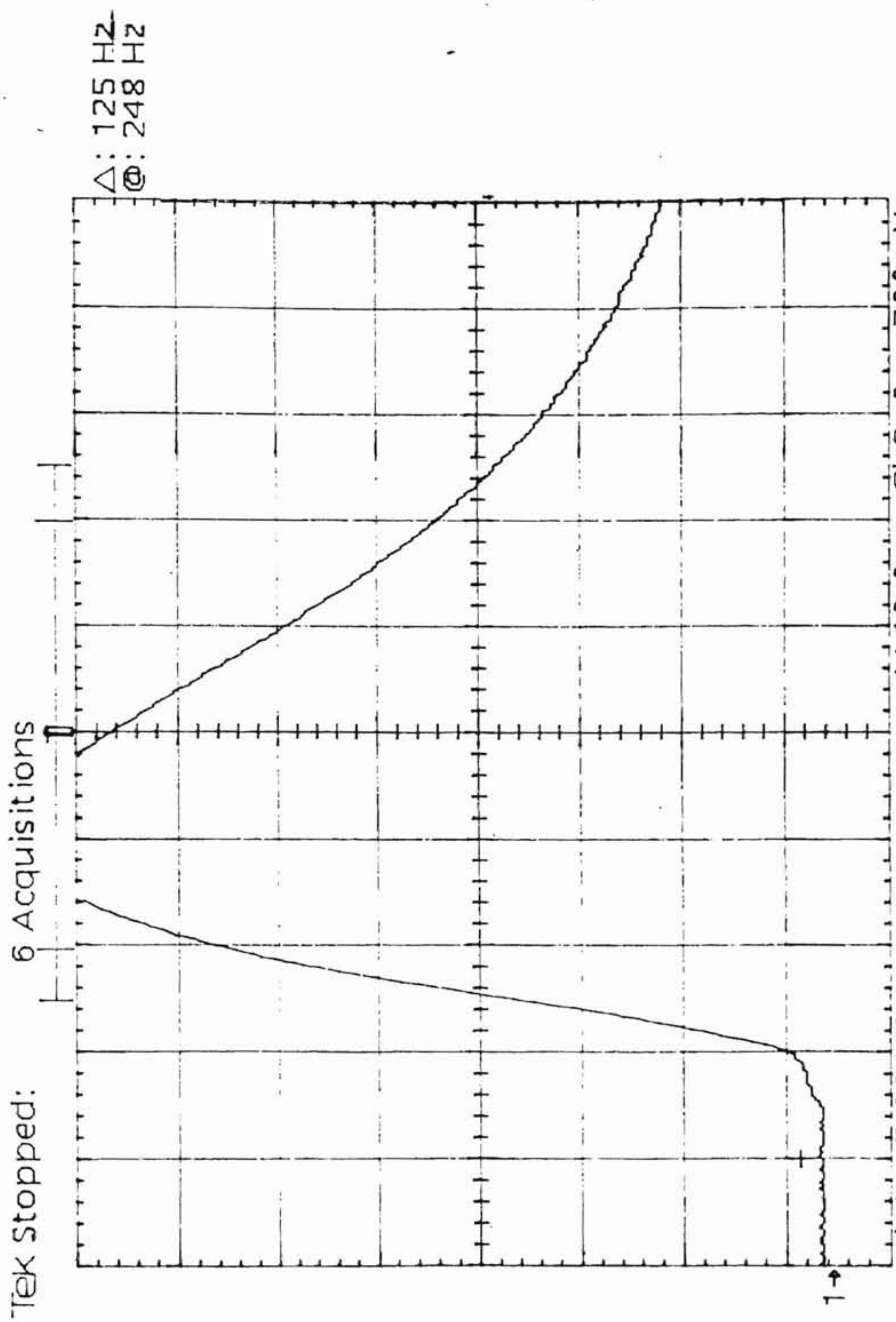

Figure 31

Flashlamp Current Pulse with one Metglass Core, 2 Loops at 800 V, with Simmer.

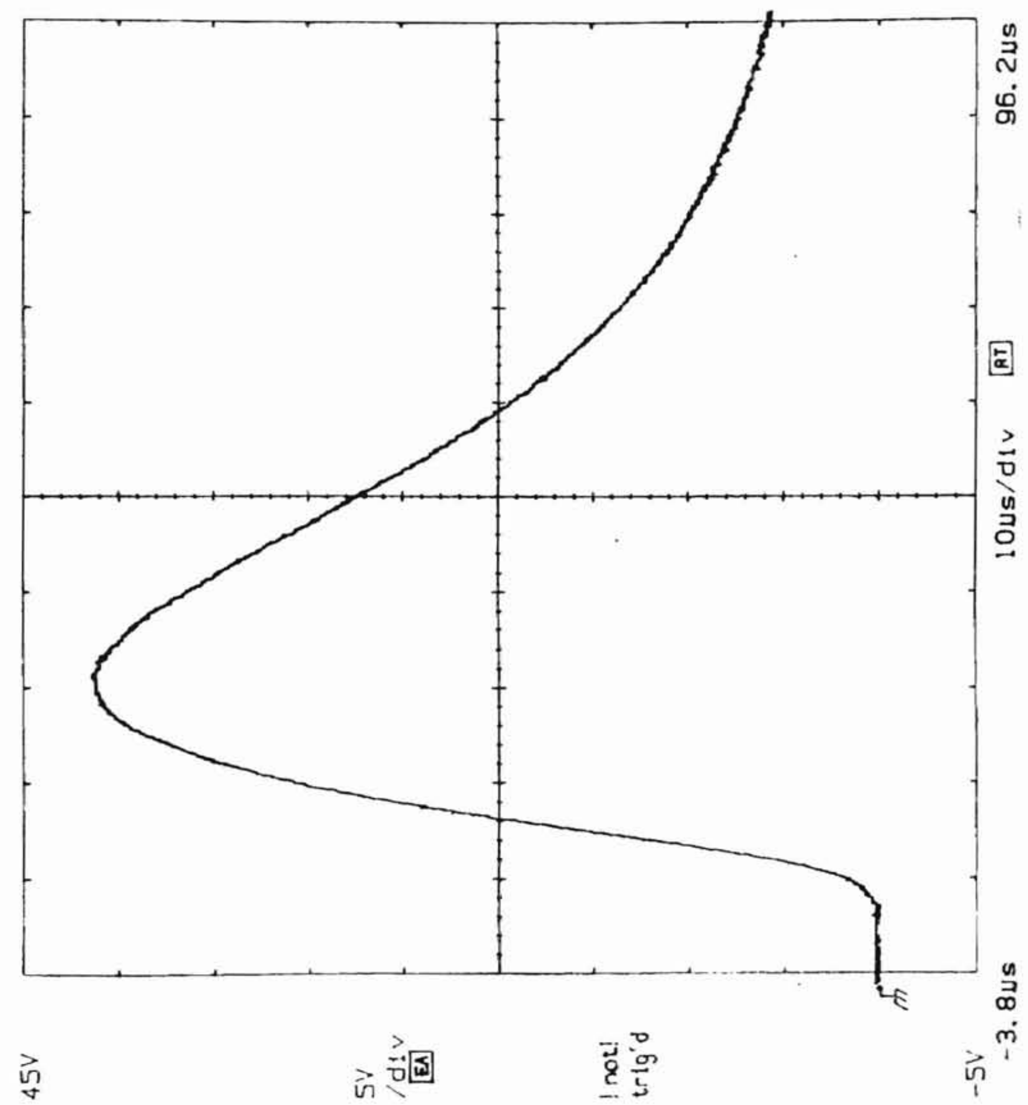

Figure 32

Flashlamp Current Pulse with Three Metglass Cores, 2 Loops at 800 V, No Simmer.

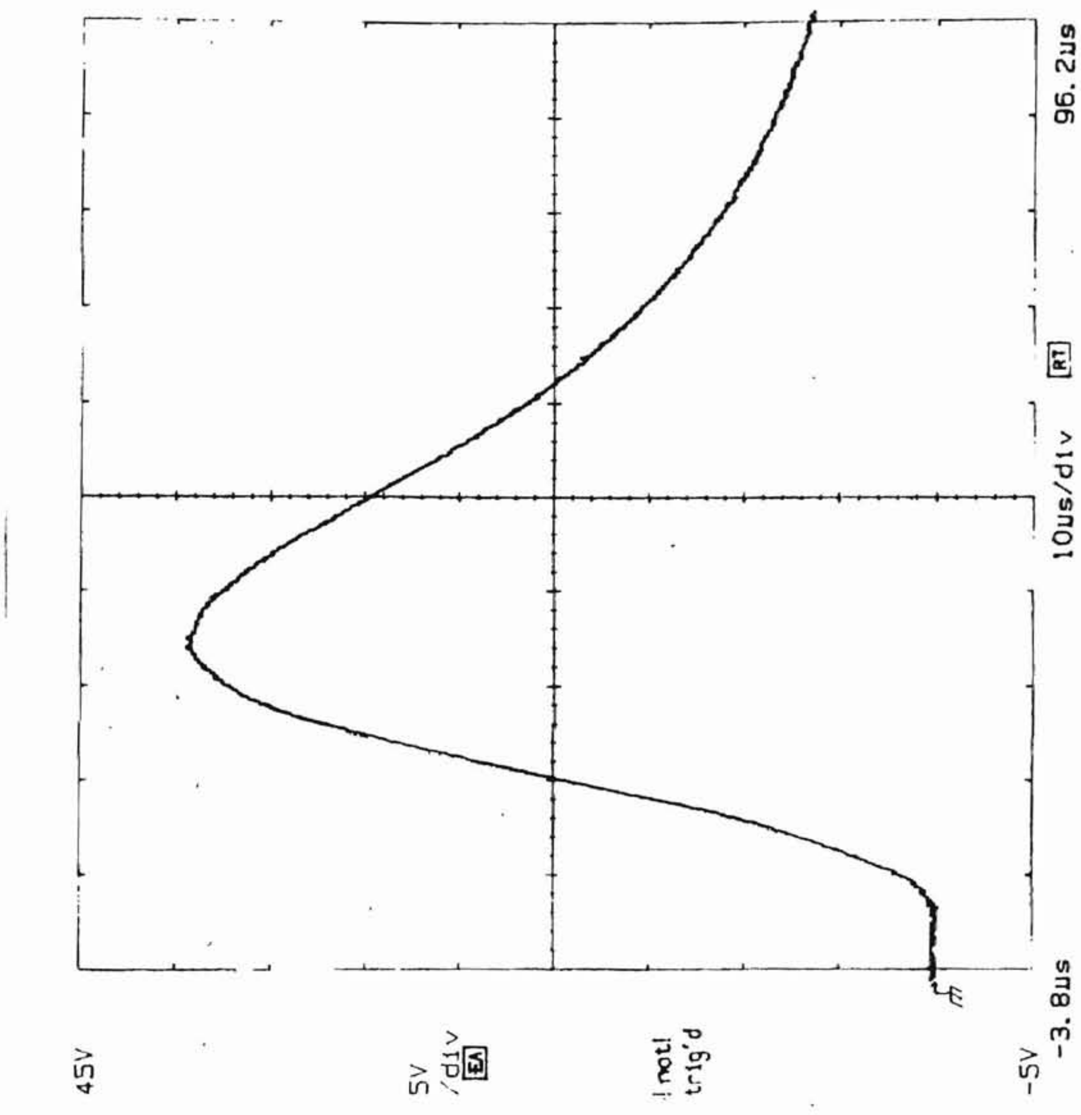

Figure 33

Flashlamp Current Pulse with Three Metglass Cores, 1 Loop at 800 V, with Simmer.

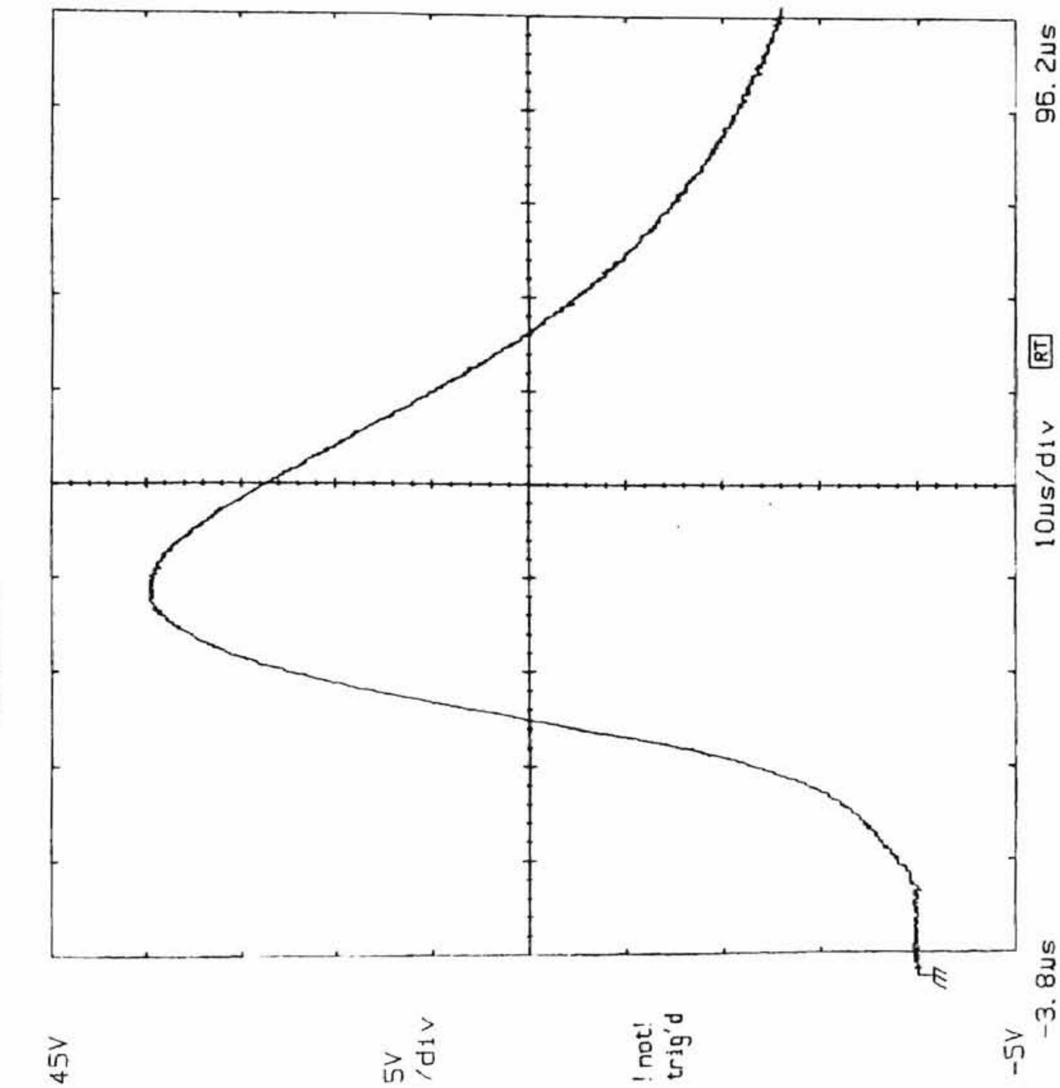

Figure 34

Flashlamp Current Pulse with Three Metglass Cores, 2 Loops at 800 V, with Simmer.

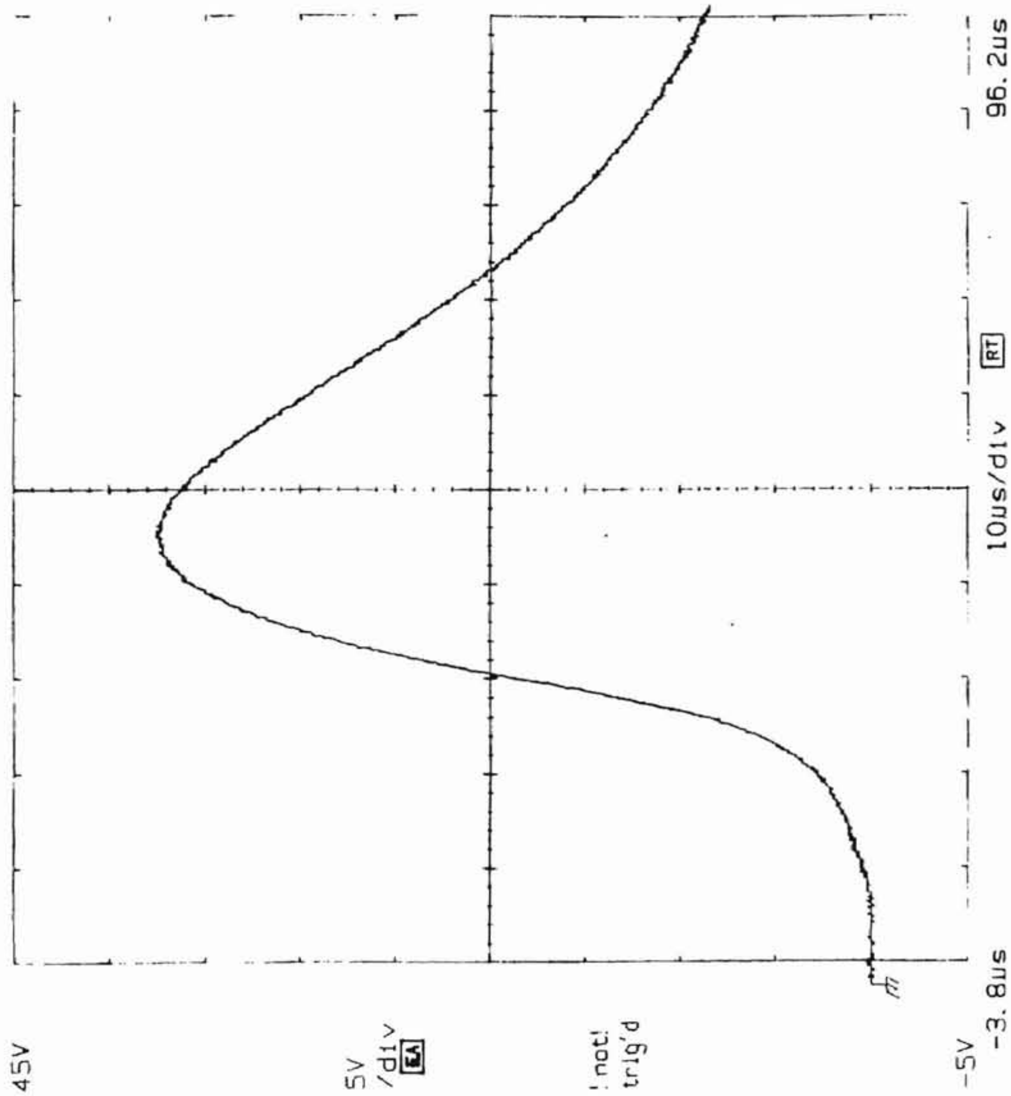

Figure 35

Flashlamp Current Pulse with Three Metglass Cores, 3 Loops at 800 V, with Simmer.

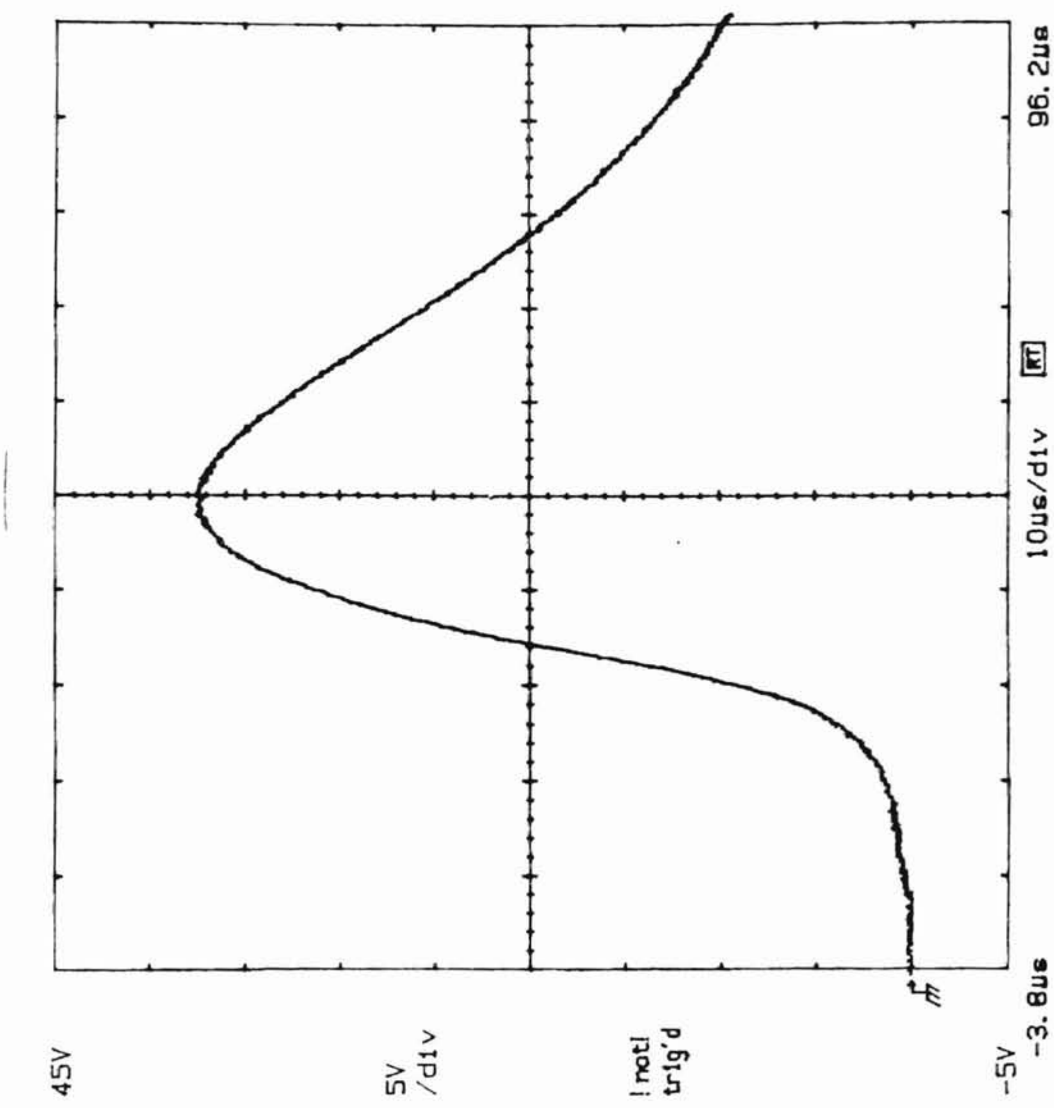

Figure 36

Flashlamp Current Pulse with Three Metglass Cores, 4 Loops at 800 V, with Simmer.

VITA

David Charles Rider

Candidate for the Degree of

Master of Science

Thesis: MEASUREMENTS OF PARAMETERS OF A FLASHLAMP PUMPED ALEXANDRITE LASER

Major Field: Electrical Engineering

Biographical:

Personal Data: Born in Syracuse, New York on July 22, 1962. The son of John C. and Mary H. Rider.

Education: Graduated from Oklahoma State University with a Bachelor of Science degree in May 1993.
Completed the requirements for the Master of Science degree at Oklahoma State University with a major in Electrical Engineering in December 1998.

Experience: Consultant, Rider Consulting Services, Inc., 1994 to present.
Research Technician, Oklahoma State University, 1992 to present.
Teaching Assistant, School of Electrical Engineering, Oklahoma State University, 1995-96.
Engineering Intern, Seagate Technologies, Inc., 1989-92.
Engineering Intern, Control Data Corporation, 1989.
Automotive Electronic and Mechanical Diagnotic Technician, ASE Master Certified, 1983-92.

Professional Memberships: International Association of Arson Investigators.
National Fire Protection Association.